

1

2 **Virus genomes from deep sea sediments expand the ocean megavirome and support 3 independent origins of viral gigantism**

4

5 Disa Bäckström^{1,*}, Natalya Yutin^{2,*}, Steffen L. Jørgensen³, Jennah Dharamshi¹, Felix Homa¹, Katarzyna
6 Zaremba-Niedwiedzka¹, Anja Spang^{1,4}, Yuri I. Wolf², Eugene V. Koonin^{2,#}, Thijs J. G. Ettema^{1,#}

7

8 ¹Department of Cell and Molecular Biology, Science for Life Laboratory, Uppsala University, Box 596,
9 Uppsala SE-75123, Sweden

10 ²National Center for Biotechnology Information, National Library of Medicine, National Institutes of Health,
11 Bethesda, MD 20894, USA

12 ³ Department of Biology, Centre for Geobiology, University of Bergen, N-5020 Bergen, Norway

13 ⁴ NIOZ, Royal Netherlands Institute for Sea Research, Department of Marine Microbiology and
14 Biogeochemistry, and Utrecht University, P.O. Box 59, NL-1790 AB Den Burg, The Netherlands

15

16 * These authors have contributed equally.

17

18 #For correspondence: koonin@ncbi.nlm.nih.gov; thijs.ettema@icm.uu.se

19

20 **Abstract**

21 The Nucleocytoplasmic Large DNA Viruses (NCLDV) of eukaryotes (proposed order "Megavirales")
22 include the families *Poxviridae*, *Asfarviridae*, *Iridoviridae*, *Ascoviridae*, *Phycodnaviridae*, *Marseilleviridae*,
23 and *Mimiviridae*, as well as still unclassified Pithoviruses, Pandoraviruses, Molliviruses and Faustoviruses.
24 Several of these virus groups include giant viruses, with genome and particle sizes exceeding those of many
25 bacterial and archaeal cells. We explored the diversity of the NCLDV in deep-sea sediments from the Loki's
26 Castle hydrothermal vent area. Using metagenomics, we reconstructed 23 high quality genomic bins of novel
27 NCLDV, 15 of which are closest related to Pithoviruses, 5 to Marseilleviruses, 1 to Iridoviruses, and 2 to
28 Klosneuviruses. Some of the identified Pitho-like and Marseille-like genomes belong to deep branches in the
29 phylogenetic tree of core NCLDV genes, substantially expanding the diversity and phylogenetic depth of the
30 respective groups. The discovered viruses have a broad range of apparent genome sizes including putative giant
31 members of the family *Marseilleviridae*, in agreement with multiple, independent origins of gigantism in
32 different branches of the NCLDV. Phylogenomic analysis reaffirms the monophyly of the Pitho-Irido-Marseille
33 branch of NCLDV. Similarly to other giant viruses, the Pitho-like viruses from Loki's Castle encode translation
34 systems components. Phylogenetic analysis of these genes indicates a greater bacterial contribution than
35 detected previously. Genome comparison suggests extensive gene exchange between members of the Pitho-like
36 viruses and *Mimiviridae*. Further exploration of the genomic diversity of "Megavirales" in additional sediment
37 samples is expected to yield new insights into the evolution of giant viruses and the composition of the ocean
38 megavirome.

39

40 **Importance**

41 Genomics and evolution of giant viruses is one of the most vigorously developing areas of virus research.
42 Lately, metagenomics has become the main source of new virus genomes. Here we describe a metagenomic
43 analysis of the genomes of large and giant viruses from deep sea sediments. The assembled new virus genomes

44 substantially expand the known diversity of the Nucleo-Cytoplasmic Large DNA Viruses of eukaryotes. The
45 results support the concept of independent evolution of giant viruses from smaller ancestors in different virus
46 branches.

47 **Introduction**

48 The nucleocytoplasmic large DNA viruses (NCLDV) comprise an expansive group of viruses that infect
49 diverse eukaryotes (1). Most of the NCLDV share the defining biological feature of reproducing (primarily) in
50 the cytoplasm of the infected cells as well as several genes encoding proteins involved in the key roles in virus
51 morphogenesis and replication, leading to the conclusion that the NCLDV are monophyletic, that is, evolved
52 from a single ancestral virus (2, 3). As originally defined in 2001, the NCLDV included 5 families of viruses:
53 *Poxviridae*, *Asfarviridae*, *Iridoviridae*, *Ascoviridae*, and *Phycodnaviridae* (2). Subsequent isolation of viruses
54 from protists has resulted in the stunning discovery of giant viruses, with genome sizes exceeding those of many
55 bacteria and archaea (4-8). The originally discovered group of giant viruses has formed the family *Mimiviridae*
56 (9-13). Subsequently, 3 additional other groups of giant viruses have been identified, namely, Pandoraviruses
57 (14-16);Pithoviruses, Cedratviruses and Orpheovirus (hereafter, the latter 3 groups of related viruses are
58 collectively referred to as the putative family "Pithoviridae") (17-19), and *Mollivirus sibericum* (20), along
59 with two new groups of NCLDV with moderate-sized genomes, the family *Marseilleviridae* (21, 22), and
60 Faustoviruses (23, 24). Most of the NCLDV have icosahedral virions composed of a double jelly roll major
61 capsid proteins but Poxviruses have distinct brick-shaped virions, ascoviruses have ovoid virions, Mollivirus
62 has a spherical virion, finally, Pandoraviruses and Pithoviruses have unusual, amphora-shaped virions.. The
63 Pithovirus virions are the largest among the currently known viruses. Several of the recently discovered groups

64 of NCLDV are likely to eventually become new families in particular, the putative ; family "Pithoviridae" (25),
65 and reclassification of the NCLDV into a new virus order "Megavirales" has been proposed (26, 27).

66 Phylogenomic reconstruction of gene gain and loss events resulted in mapping about 50 genes that are
67 responsible for the key viral functions to the putative last common ancestor of the NCLDV, reinforcing the
68 conclusion on their monophyly (3, 28). However, detailed phylogenetic analysis of these core genes of the
69 NCLDV has revealed considerable evolutionary complexity including numerous cases of displacement of
70 ancestral genes with homologs from other sources, and even some cases of independent capture of homologous
71 genes (29). The genomes of the NCLDV encompass from about 100 (some iridoviruses) to nearly 2500 genes
72 (pandoraviruses) that, in addition to the 50 or so core genes, include numerous genes involved in various
73 aspects of virus-host interaction, in particular, suppression of the host defense mechanisms, as well as many
74 genes for which no function could be identified (1, 30).

75 The NCLDV include some viruses that are agents of devastating human and animal diseases, such as
76 smallpox virus or African swine fever virus (31, 32), as well as viruses that infect algae and other planktonic
77 protists and are important ecological agents (12, 33-35). Additionally, NCLDV elicit strong interest of many
78 researchers due to their large genome size which, in the case of the giant viruses, falls within the range of
79 typical genome size of bacteria and archaea. This apparent exceptional position of the giant viruses in the
80 virosphere, together with the fact that they encode multiple proteins that are universal among cellular
81 organisms, in particular, translation system components, has led to provocative scenarios of the origin and

82 evolution of giant viruses. It has been proposed that the giant viruses were descendants of a hypothetical,
83 probably, extinct fourth domain of cellular life that evolved via drastic genome reduction, and support of this
84 scenario has been claimed from phylogenetic analysis of aminoacyl-tRNA synthetases encoded by giant viruses
85 (5, 26, 36-40). However, even apart from the conceptual difficulties inherent in the postulated cell to virus
86 transition (41, 42), phylogenetic analysis of expanded sets of translation-related proteins encoded by giant
87 viruses has resulted in tree topologies that were poorly compatible with the fourth domain hypothesis but rather
88 suggest piecemeal acquisition of these genes, likely, from different eukaryotic hosts (43-46).

89 More generally, probabilistic reconstruction of gene gains and losses during the evolution of the
90 NCLDV has revealed a highly dynamic evolutionary regime (3, 28, 29, 45, 46) that has been conceptualized in
91 the so-called genomic accordion model under which virus evolution proceeds via alternating phases of
92 extensive gene capture and gene loss (47, 48). In particular, in the course of the NCLDV evolution, giant
93 viruses appear to have evolved from smaller ones on multiple, independent occasions (45, 49, 50).

94 In recent years, metagenomics has become the principal route of new virus discovery (51-53). However,
95 in the case of giant viruses, *Acanthamoeba* co-culturing has remained the main source of new virus
96 identification, and this methodology has been refined to allow for high-throughput giant virus isolation (54, 55).
97 To date, over 150 species of giant viruses have been isolated from various environments, including water
98 towers, soil, sewage, rivers, fountains, seawater, and marine sediments (56). The true diversity of giant viruses
99 is difficult to assess, but the explosion of giant virus discovery during the last ten years, and large scale
100 metagenomic screens of viral diversity indicates that a major part of the Earth's virome remains unexplored
101 (57). The core genes of the NCLDV can serve as baits for screening environmental sequences, and pipelines

102 have been developed for large scale screening of metagenomes (56, 58). Although these efforts have given
103 indications of the presence of uncharacterized giant viruses in samples from various environments, few of these
104 putative novel viruses can be characterized due to the lack of genomic information. Furthermore, giant viruses
105 tend to be overlooked in viral metagenomic studies since samples are typically filtered according to the
106 preconception of typical virion sizes (52).

107 To gain further insight into the ecology, evolution, and genomic content of giant viruses, it is necessary
108 to retrieve more genomes, not simply establish their presence by detection of single marker genes.

109 Metagenomic binning is the process of clustering environmental sequences that belong to the same genome,
110 based on features such as base composition and coverage. Binning has previously been used to reconstruct the
111 genomes of large groups of uncharacterized bacteria and archaea in a culture-independent approach (59, 60).
112 Only one case of binning has been reported for NCLDV, when the genomes of the Klosneuviruses, distant
113 relatives of the Mimiviruses, were reconstructed from a simple wastewater sludge metagenome (46). More
114 complex metagenomes from all types of environments remain to be explored. However, standard methods for
115 screening and binning of NCLDV have not yet been developed, and sequences of these viruses can be difficult
116 to classify because of substantial horizontal gene transfer from bacteria and eukaryotes (13, 29, 43, 49), and also
117 because a large proportion of the NCLDV genes (known as ORFans) have no detectable homologs (25, 30).

118 We identified NCLDV sequences in deep sea sediment metagenomes from Loki's Castle, a sample site
119 that has been previously shown to be rich in uncharacterized prokaryotes (61, 62) (Dharamshi et. al. 2018
120 (submitted)). The complexity of the data and genomes required a combination of different binning methods,
121 assembly improvement by reads profiling, and manual refinement of each bin to minimize contamination with
122 non-viral sequences. As a result, 23 high quality genomic bins of novel NCLDV were reconstructed, including,
123 mostly, distant relatives of "Pithoviridae", Orpheovirus, and *Marseilleviridae*, as well as two relatives of
124 Klosneuviruses. These findings substantially expand the diversity of the NCLDV, in particular, the Pitho-Irido-

125 Marseille (PIM) branch, further support the scenario of independent evolution of giant viruses from smaller
126 ones in different branches of the NCLDV, and provide an initial characterization of the ocean megavirome.
127

128

129 Materials and Methods

130

131 Sampling and metagenomic sequencing

132 In the previous studies of microbial diversity in the deep sea sediments, samples were retrieved from three sites
133 about 15 km north east of the Loki's castle hydrothermal vent field (Table S1 of Additional File 1), by gravity
134 (GS10_GC14, GS08_GC12) and piston coring (GS10_PC15) (61, 63, 64).

135

136 DNA was extracted and sequenced, and metagenomes were assembled as part of the previous studies ((61) for
137 GS10_GC14, Dharamshi et. al. 2018 (submitted) for GS08_GC12 and GS10_PC15), resulting in the assemblies
138 LKC75, KR126, K940, K1000, and K1060. Contiguous sequences (contigs) longer than 1kb were selected for
139 further processing.

140

141 Identification of viral metagenomic sequences

142 Protein sequences of the metagenomic contigs were predicted using Prodigal v.2.6.3 (65), in the metagenomics
143 mode. A collection of DNA polymerase family B (DNAP) sequences from 11 NCLDV was used to query the
144 metagenomic protein sequence with BLASTP ((66), Table S1 of Additional File 1). The BLASTP hits were
145 filtered according to e-value (maximum 1e⁻⁵), alignment length (at least 50% of the query length) and identity
146 (greater than 30%). The sequences were aligned using MAFFT-LINSI (67). Reference NCLDV DNAP
147 sequences were extracted from the NCVOG collection (28). Highly divergent sequences and those containing
148 large gaps inserts were removed from the alignment, followed by re-alignment. The terminal regions of the

149 alignments were trimmed manually using Jalview (68), and internal gaps were removed using trimAl
150 (v.1.4.rev15, (69)) with the option “gappyout”. IQTree version 1.5.0a (70) was used to construct maximum
151 likelihood phylogenies with 1000 ultrafast bootstrap replications (71). The built-in model test (72) was used to
152 select the best evolutionary model according to the Bayesian information criterion (LG+F+I+G4; Figure S1 of
153 Additional File 1). Contigs belonging to novel NCLDVs were identified and used for binning.

154

155 **Composition-based binning (ESOM)**

156 All sequences of the assemblies KR126, K940, K1000 and K1060 were split into fragments of minimum 5 or
157 10 kb length at intervals of 5 or 10 kb, and clustered by tetranucleotide frequencies using Emergent Self
158 Organizing maps (ESOM, (73)), generating one map per assembly. Bins were identified by viewing the maps
159 using Databionic ESOM viewer (<http://databionic-esom.sourceforge.net/>), and manually choosing the contigs
160 clustering together with the putative NCLDV contigs in an “island” (Figure S3 of Additional File 1).

161

162 **Differential coverage binning of metagenomic contigs**

163 Differential coverage (DC) bins were generated for the KR126, K940, K1000, and K1060 metagenomes,
164 according to Dharamshi et. al. 2018 (submitted). Briefly, Kallisto version 0.42.5 (74) was used to get the
165 differential coverage data of each read mapped onto each focal metagenome, that was used by CONCOCT
166 version 0.4.1 to collect sequences into bins (75). CONCOCT was run with three different contig size thresholds:
167 2kb, 3kb, and 5kb, and longer contigs were cut up into smaller fragments (10 kb), to decrease coverage and
168 compositional bias, and merged again after CONCOCT binning (See Dharamshi et. al. 2018 (submitted) for
169 further details). Bins containing contigs with the viral DNAP were selected and refined in mmgenome (76).
170 Finally, to resolve overlapping sequences in the DC bins, the reads of each bin were extracted using seqtk
171 (version 1.0-r82-dirty, <https://github.com/lh3/seqtk>) and the reads mapping files generated for mmgenome, and

172 reassembled using SPAdes (3.6.0, multi-cell, --careful mode, (77)). Bins from KR126 had too low coverage and
173 quality, and were discarded from further analysis.

174

175 **Co-assembly binning of metagenomic contigs**

176 CLARK (78), a program for classification of reads using discriminative k-mers, was used to identify reads
177 belonging to NCLDV in the metagenomes. A target set of 10 reference genomes that represented
178 Klosneuviruses, *Marseilleviridae*, and "Pithoviridae" (Table S2 of Additional File 1), as well as the 29 original
179 bins, were used to make a database of spaced k-mers which CLARK used to classify the reads of the K940,
180 K1000 and K1060 metagenomes (full mode, k-mer size 31). Reads classified as related to any of the targets
181 were extracted and the reads from all three metagenomes were pooled and reassembled using SPAdes (3.9.0,
182 (77)). Because CLARK removes not-discriminatory k-mers, the reads for sequences that are similar between
183 the bins might not have been included. Therefore, the reads from each original bin that were used for the first
184 set reassemblies, were also included, and pooled with the CLARK-classified reads before reassembly.

185

186 Four SPAdes modes were tested: metagenomic (--meta), single-cell (--sc), multi-cell (default), and multi-cell
187 careful (--careful). The quality of the assemblies was tested by identifying the contigs containing NCVOG0038
188 (DNA polymerase), using BLASTP (66). The multi-cell careful assembly had the longest DNAP-containing
189 contigs and was used for CONCOCT binning.

190

191 CONCOCT was run as above, only using reads from the co-assembly as input. Bins containing NCVOG0038
192 were identified by BLASTP. The smaller the contig size threshold, the more ambiguous and potentially
193 contaminating sequences were observed, so the CONCOCT 5 kb run was chosen to extract and refine new bins.
194 The bins were refined by using mmgenome as described below.

195

196 **Quality assessment and refinement of metagenomic NCLDV bins**

197 General sequence statistics were calculated by Quast (v. 3.2 , (79)). Barrnap (v 0.8; (80)) was used to check for
198 the presence of rRNA genes, with a length threshold of 0.1. Prokka (v1.12, (79)) was used to annotate open
199 reading frames (ORFs) of the raw bins. Megavirus marker gene presence in each metagenomic bin was
200 estimated by using the micomplete pipeline (<https://bitbucket.org/evolegiolab/micomplete>) and a set of the 10
201 conserved NCLDV genes (Table S3 of Additional File 1). This information was used to assess completeness
202 and redundancy. Presence of more than one copy of each marker gene was considered an indication of potential
203 contamination or the presence of more than one viral genome per bin, and such bins were further refined.

204

205 Mmgenome was used to manually refine the metagenomic bins by plotting coverage and GC-content, showing
206 reads linkage, and highlighting contigs with marker genes (76). Overlap between the ESOM binned contigs and
207 the DC bins was also visualized. Bins containing only one genome were refined by removing contigs with
208 different composition and coverage. In cases when several genomes were represented in the same CONCOCT
209 bin, they were separated into different bins when distinct clusters were clearly visible (see the Supplementary
210 Materials of Additional File 1 for examples of the refining process).

211 Reads linkage was determined by mapping the metagenomic reads onto the assembly using bowtie2 (version
212 2.3.2, (81)), samtools (version 1.2, (82)) to index and convert the mapping file into bam format, and finally a
213 script provided by the CONCOCT suite to count the number of read pairs that were mapping to the first or last 1
214 kb of two different contigs (bam_to_linkage.py, --regionlength 1000).

215

216 Diamond aligner Blastp (83) was used to query the protein sequences of the refined bins against the NCBI non-
217 redundant protein database (latest date of search: Febuary 13 2018), with maximum e-value 1e⁻⁵. Taxonomic
218 information from the top BLASTP hit for each gene was used for taxonomic filtering. Contigs were identified

219 as likely contaminants and removed if they had 50% or more bacterial or archaeal hits compared to no
220 significant hits, and no viral or eukaryotic hits.

221
222 The assemblies of the DC and CA bins were compared by aligning the contigs with nucmer (part of
223 MUMmer3.23,(84)) and an in-house script for visualization (see Additional File 1 for more details).
224
225

226 **Assessment of NCLDV diversity**

227 Environmental sequences, downloaded in March 2017 from TARA Oceans ((85),
228 <https://www.ebi.ac.uk/ena/about/tara-oceans-assemblies>), and EarthVirome ((57), available at
229 <https://img.jgi.doe.gov/vr/>) were combined with the metagenomic sequences from Loki's Castle (Table S1 of
230 Additional file 1) and screened for sequences related to the Loki's Castle NCLDVs using BLASTP search with
231 the bin DNAP sequences as queries. The BLASTP hits were filtered according to e-value (maximum 1e⁻⁵), HSP
232 length (at least 50% of the query length) and identity above 30%. The sequences were extracted using
233 blastdbcmd, followed by alignment and phylogenetic tree reconstruction as described above (Figure 1).
234

235 **Sequence annotation and phylogenetic analysis**

236 The sequences of the selected bins were translated with MetaGeneMark (86). tRNA genes were predicted using
237 tRNAscan-SE online (87). Predicted proteins were annotated using their best hits to NCVOG, cdd, and *nr*
238 databases. In addition, Pitho-, Marseille-, Iridovirus-related bins were annotated using protein clusters
239 constructed as described below. Reference sequences were collected from corresponding NCVOG and cdd
240 profiles, and from GenBank, using BLASTP searches initiated from the Loki's Castle NCLDV proteins.
241 Reference sequences for Loki's Castle virophages were retrieved by BLAST and tBLASTn searches against
242 genomic (nr) and metagenomic (environmental wgs) parts of GenBank, with the predicted Loki's Castle

243 virophage MCP as queries. The retrieved environmental virophage genome fragments were translated with
244 MetaGeneMark. Homologous sequences were aligned using MUSCLE (88). For phylogenetic reconstruction,
245 gapped columns (more than 30% of gaps) and columns with low information content were removed from the
246 alignments (89); the filtered alignments were used for tree reconstructions using FastTree (90). The alignments
247 of three conserved NCLDV proteins were concatenated and used for phylogenetic analysis with PhyML ((91),
248 <http://www.atgc-montpellier.fr/phymml-sms/>) The best model identified by PhyML was LG +G+I+F (LG
249 substitution model, gamma distributed site rates with gamma shape parameter estimated from the alignment;
250 fraction of invariable sites estimated from the alignment; and empirical equilibrium frequencies).

251

252 Protein sequence clusters

253 Two sets of viral proteins, Pitho-Irido-Marseillevirus group (PIM clusters,
254 ftp://ftp.ncbi.nih.gov/pub/yutinn/Loki_Castle_NCLDV_2018/PIM_clusters/) and NCLDV (NCLDV clusters,
255 ftp://ftp.ncbi.nih.gov/pub/yutinn/Loki_Castle_NCLDV_2018/NCLDV_clusters/) were used separately to obtain
256 two sets of protein clusters, using an iterative clustering and alignment procedure, organized as follows

257

- 258 • ***initial sequence clustering:*** Initially, sequences were clustered using UCLUST (92) with the similarity
259 threshold of 0.5; clustered sequences were aligned using MUSCLE, singletons were converted to
260 pseudo-alignments consisting of just one sequence. Sites containing more than 67% of gaps were
261 temporarily removed from alignments and the pairwise similarity scores were obtained for clusters
262 using HHSEARCH. Scores for a pair of clusters were converted to distances [the
263 $d_{A,B} = -\log(s_{A,B}/\min(s_{A,A}, s_{B,B}))$ formula was used to convert scores s to distances d] a UPGMA guide
264 tree was produced from a pairwise distance matrix. A progressive pairwise alignment of the clusters at
265 the tree leaves was constructed using HHALIGN (93), resulting in larger clusters. The procedure was
repeated iteratively, until all sequences with detectable similarity over at least 50% of their lengths

266 were clustered and aligned together. Starting from this set of clusters, several rounds of the following
267 procedures were performed.

268 • ***cluster merging and splitting:*** PSI-BLAST (94) search using the cluster alignments to construct
269 Position-Specific Scoring Matrices (PSSMs) was run against the database of cluster consensus
270 sequences. Scores for pairs of clusters were converged to a distance matrix as described above;
271 UPGMA trees were cut using at the threshold depth; unaligned sequences from the clusters were
272 collected and aligned together. An approximate ML phylogenetic tree was constructed from each of
273 these alignments using FastTree (WAG evolutionary model, gamma-distributed site rates). The tree
274 was split into subtrees so as to minimize paralogy and maximize species (genome) coverage.
275 Formally, for a subtree containing k genes belonging to m genomes ($k \geq m$) in the tree with the total of
276 n genomes ($n \geq m$) genomes, the “autonomy” value was calculated as $(m/k)(m/n)(a/b)^{1/6}$ (where a is the
277 length of the basal branch of the subtree and b is the length of the longest internal branch in the entire
278 tree). This approach gives advantage to subtrees with the maximum representation of genomes,
279 minimum number of paralogs and separated by a long internal branch. If a subtree with the maximum
280 autonomy value was different from the complete tree, it was pruned from the tree, recorded as a
281 separate cluster, and the remaining tree was analyzed again.
282 • ***cluster cutting and joining:*** Results of PSI-BLAST search whereby the cluster alignments were used
283 as PSSMS and run against the database of cluster consensus sequences were analyzed for instances
284 where a shorter cluster alignment had a full-length match to a longer cluster containing fewer
285 sequences. This situation triggered cutting the longer alignment into fragments matching the shorter
286 alignment(s). Alignment fragments were then passed through the merge-and-split procedure described
287 above. If the fragments of the cluster that was cut did not merge into other clusters, the cut was rolled
288 back, and the fragments were joined.

289

- ***cluster mapping and realigning:*** PSI-BLAST search using the cluster alignments as PSSMs was run
290 against the original database. Footprints of cluster hits were collected, assigned to their respective
291 highest-scoring query cluster and aligned, forming the new set of clusters mirroring the original set.
- ***post-processing:*** The PIM group clusters were manually curated and annotated using the NCVOG,
292 CDD and HHPRED matches as guides. For the NCLDV clusters, the final round clusters with strong
293 reciprocal PSI-BLAST hits and with compatible phyletic patterns (using the same autonomy value
294 criteria as described above) were combined into clusters of homologs that maximized genome
295 representation and minimized paralogy. The correspondence between the previous version of
296 NCVOGs and the current clusters was established by running PSI-BLAST with the NCVOG
297 alignments as PSSMs against the database of cluster consensus sequences.

298

299 **Genome similarity dendrogram**

300 Binary phyletic patterns of the NCLDV clusters (whereby 1 indicates a presence of the given cluster in the
301 given genome) were converted to intergenomic distances as follows: $d_{X,Y} = -\log(N_{X,Y}/(N_X N_Y)^{1/2})$ where N_X and N_Y
302 are the number of COGs present in genomes X and Y respectively and $N_{X,Y}$ is the number of COGs shared by
303 these two genomes. A genome similarity dendrogram was reconstructed from the matrix of pairwise distances
304 using the Neighbor-Joining method (95).

305 **Conserved motif search**

306 The sequences from the LCV genomic bins were searched for potential promoters as follows. For every
307 predicted ORF, ‘upstream’ genome fragments (from 250 nucleotides upstream to 30 nucleotides downstream of
308 the predicted translation start codons) were extracted; short fragments (less than 50 nucleotides) were excluded;
309 the resulting sequence sets were searched for recurring ungapped motifs using MEME software, with motif
310 width set to either 25, 12, or 8 nucleotides (96). The putative LCV virophage promoter was used as a template

311 to search upstream fragments of LCMiAC01 and LCMiAC02 with FIMO online tool (96). The motifs were
312 visualized using the Weblogo tool (97).

313

314 **Data availability**

315 The nucleotide sequences reported in this work have been deposited in GenBank under the accession numbers
316 X00001-X0000N.

317 **Results**

318
319 **Putative NCLDV in the Loki's Castle metagenome**
320

321 Screening of the Loki's Castle metagenomes, for NCLDV DNA polymerase sequences revealed remarkable
322 diversity (Figure 1, Figure S2, Additional File 1). Using two main binning approaches, namely, differential
323 coverage binning (DC), and co-assembly binning (CA) (Figure 2), we retrieved 23 high quality bins of putative
324 new NCLDVs (Table 1). The highest quality bins were identified by comparing the DC and the CA bins, based
325 on decreasing the total number of contigs and the number of contigs without NCLDV hits, while preserving
326 completeness (Additional File 1, Table S6).

327
328 Differential coverage binning was performed first, resulting in 29 genomic bins. Initial quality assessment
329 showed that most of the bins were inflated and fragmented, containing many short contigs (<5kb), which were
330 difficult to classify as contamination or *bona fide* NCLDV sequences, and some bins were likely to contain
331 sequences from more than one viral genome, judged by the presence of marker genes belonging to different
332 families of the NCLDV (Additional file 1, Figures S19-S20). The more contigs a bin contains, the higher the
333 risk is that some of these could be contaminants that bin together because of similar nucleotide composition and
334 read coverage. Therefore, sequence read profiling followed by co-assembly binning was performed in an
335 attempt to increase the size of the contigs and thus obtain additional information for binning and bin refinement.
336 For most of the bins, the co-assembly led to a decrease in the number of contigs, without losing completeness or
337 even improving it (Additional file 1, Table S6).

338
339 A key issue with metagenomic binning is whether contigs are binned together because they belong to the same
340 genome, or rather because they simply display a similar nucleotide composition and read coverage. In general,

341 contigs were retained if they contained at least one gene with BLASTP top hits to NCLDV proteins. Some
342 contigs encoded proteins with only bacterial, archaeal, and/or eukaryotic BLASTP top hits, and because the
343 larger NCLDV genomes contain islands enriched in genes of bacterial origin (43, 49), it was unclear which
344 sequences could potentially be contaminants. A combination of gene content, coverage and composition
345 information was used to identify potential contaminating sequences. Contigs shorter than 5 kb were also
346 discarded because they generally do not contain enough information to reliably establish their origin, but this
347 strict filtering also means that the size of the genomes could be underestimated and some genomic information
348 lost. Reassuringly, no traces of ribosomal RNA or ribosomal protein genes were identified in any of the
349 NCLDV genome bins, which would have been a clear case of contaminating cellular sequences. Altogether, of
350 the 336 contigs in the 23 final genome bins, 243 (72%) could be confidently assigned to NCLDV on the basis of
351 the presence of at least one NCLDV-specific gene.

352

353 The content of the 23 NCLDV-related bins was analyzed in more depth (Table 1). The bins included from 1 to
354 30 contigs, with the total length of non-overlapping sequences varying from about 200 to more than 750
355 kilobases (kb), suggesting that some might contain (nearly) complete NCLDV genomes although it is difficult
356 to make any definitive conclusions on completeness from length alone because the genome size of even closely
357 related NCLDV can vary substantially. A much more reliable approach is to assess the representation of core
358 genes that are expected to be conserved in (nearly) all NCLDV. The translated protein sequences from the 23
359 bins were searched for homologs of conserved NCLDV genes using PSI-BLAST, with profiles of the NCVOGs
360 employed as queries ((28); see Additional File 2 for protein annotation). Of the 23 bins, in 14 (nearly) complete
361 sets of the core NCLDV genes were identified (Table 1) suggesting that these bins contained (nearly) complete
362 genomes of putative new viruses (hereafter, LCV, Loki's Castle Viruses). Notably, the Pithovirus-like LCV
363 lack the packaging ATPase of the FtsK family that is encoded in all other NCLDV genomes but not in the
364 available Pithovirus genomes. Several bins contained more than one copy of certain conserved genes. Some of

365 these could represent actual paralogs but, given that duplication of most of these conserved genes (e.g. DNA
366 Polymerase in Bin LCPAC202 or RNA polymerase B subunit in Bins LCPAC201 and LCPAC202) is
367 unprecedented among NCLDV, it appears likely that several bins are heterogeneous, each containing sequences
368 from two closely related virus genomes.

369 With all the caution due because of the lack of fully assembled virus genomes, the range of the apparent
370 genomes sizes of the Pitho-like and Marseille-like LCV is notable (Table 1). The characteristic size of the
371 genomes in the family "Pithoviridae" is about 600 kb (17-19) but, among the Pitho-like LCV, only one,
372 LCPAC304, reached and even exceeded that size. The rest of the LCV genomes are substantially smaller, and
373 although some are likely to be incomplete, given that certain core genes are missing, others, such as
374 LCPAC104, with the total length of contigs at only 218 kb, encompass all the core genes (Table 1).

375 The typical genome size in the family *Marseilleviridae* is between 350 and 400 kb (22) but among the LCV,
376 genomes of two putative Marseille-like viruses, LCMAC101 and LCMAC202, appear to exceed 700 kb, well
377 into the giant virus range. Although LCMAC202 contains two uncharacteristic duplications of core genes,
378 raising the possibility of heterogeneity, LCMAC101 contains all core genes in a single copy, and thus, appears
379 to be an actual giant virus. Thus, the family *Marseilleviridae* seems to be joining the NCLDV families that
380 evolved virus gigantism.

381
382 A concatenation of the three most highly conserved proteins, namely, NCLDV major capsid protein (MCP),
383 DNA polymerase (DNAP), and A18-like helicase (A18Hel), was used for phylogenetic analysis (see Methods
384 for details). Among the putative new NCLDV, 15 cluster with Pithoviruses (Figure 3). These new
385 representatives greatly expand the scope of the family "Pithoviridae". Indeed, 8 of the 15 form a putative
386 (weakly supported) clade that is the sister group of all currently known "Pithoviridae" (Pithovirus, Cedratvirus

387 and Orpheovirus), 5 more comprise a deeper clade, and LCDPAC02 represents the deepest lineage of the Pitho-
388 like viruses (Figure 3). Additionally, 5 of the putative new NCLDV are affiliated with the family
389 *Marseilleviridae*, and similarly to the case of Pitho-like viruses, two of these comprise the deepest branch in the
390 Marseille-like subtree (although the monophyly of this subtree is weakly supported) (Figure 3). Another LCV
391 represents a distinct lineage within the family *Iridoviridae* (Figure 3). The topologies of the phylogenetic trees
392 for individual conserved NLCDV genes were mostly compatible with these affinities of the putative new
393 viruses (Additional File 3). Taken together, these findings substantially expand the Pitho-Irido-Marseille (PIM)
394 clade of the NCLDV, and the inclusion of the LCV in the phylogeny confidently reaffirms the previously
395 observed monophyly of this branch (Figure 3). Finally, two LCV belong to the Klosneuvirus branch (putative
396 subfamily “Klosneuvirinae”) within the family *Mimiviridae* (Figure 3, inset).

397

398

399 **Translation system components encoded by Loki’s Castle viruses**

400

401 Similar to other NCLDV with giant and large genomes, the LCV show a patchy distribution of genes coding
402 for translation system components. Such genes were identified in 11 of the 23 bins (Table 2; Additional File 2).
403 None of the putative new viruses has a (near) complete set of translation-related genes (minus the ribosome) as
404 observed in Klosneuviruses (46) or Tupanviruses (98). Nevertheless, several of the putative Pitho-like viruses
405 encode multiple translation-related proteins, e.g. Bin LCMAC202 that encompasses 6 aminoacyl-tRNA
406 synthetases (aaRS) and 6 translation factors or Bin LCMAC201, with 4 aaRS and 5 translation factors (Table
407 2). Additionally, 12 of the 23 bins encode predicted tRNAs, up to 22 in Bin LCMAC202 (Table 2).

408

409 Given the special status of the translation system components in the discussions of the NCLDV evolution, we
410 constructed phylogenies for all these genes including the LCV and all other NCLDV. The results of this
411 phylogenetic analysis (Figure 4 and Additional File 3) reveal complex evolutionary trends some of which that

412 have not been apparent in previous analyses of the NCLDV evolution. First, in most cases when multiple LCV
413 encompass genes for homologous translation system components, phylogenetic analysis demonstrates
414 polyphyly of these genes. Notable examples include translation initiation factor eIF2b, aspartyl/asparaginyl-
415 tRNA synthetase (AsnS), tyrosyl-tRNA synthetase (TyrS) and methionyl-tRNA synthetase (MetS; Figure 4).
416 Thus, the eIF2b tree includes 3 unrelated LCV branches one of which, not unexpectedly, clusters with
417 homologs from Marseilleviruses and Mimiviruses, another one is affiliated with two Klosneuviruses, and the
418 third one appears to have an independent eukaryotic origin (Figure 4a). The AsnS tree includes a group of LCV
419 that clusters within a mixed bacterial and archaeal branch that also includes two other NCLDV, namely,
420 Hokovirus of the Klosneuvirus group and a phycodnavirus. Another LCV AsnS belongs to a group of apparent
421 eukaryotic origin and one, finally, belongs to a primarily archaeal clade (Figure 4b and Additional File 3). Of
422 the 3 TyrS found in LCV, two cluster with the homologs from Klosneuviruses within a branch of apparent
423 eukaryotic origin, and the third one in another part of the same branch where it groups with the Orpheovirus
424 TyrS; notably, the same branch includes homologs from pandoraviruses (Figure 4c). Of the two MetS, one
425 groups with homologs from Klosneuviruses whereas the other one appears to be of an independent eukaryotic
426 origin (Figure 4d). These observations are compatible with the previous conclusions on multiple, parallel
427 acquisitions of genes for translation system components by different groups of NCLDV (primarily, giant viruses
428 but, to a lesser extent, also those with smaller genomes), apparently, under evolutionary pressure for modulation
429 of host translation that remains to be studied experimentally.
430

431 Another clear trend among the translation-related genes of the Pitho-like LCV is the affinity of several of
432 them with homologs from Klosneuviruses and, in some cases, Mimiviruses. All 4 examples mentioned about
433 include genes of this provenance, and additional cases are GlyS, IleS, ProS, peptidyl-tRNA hydrolase,
434 translation factors eIF1a and eIF2a, and peptide chain release factor eRF1 (Additional File 3). Given that the
435 LCV set includes two Klosneuvirus-like bins, in addition to the Pitho-like ones, these observations imply

436 extensive gene exchange between distinct NCLDV in the habitats from which these viruses originate.
437 Klosneuviruses that are conspicuously rich in translation-related genes might serve as the main donors.
438
439

440 **Gene content analysis of the Loki's Castle viruses**

441 Given that the addition of the LCV has greatly expanded the family *Marseilleviridae* and the Pithovirus
442 group, and reaffirmed the monophyly of the PIM branch of NCLDV, we constructed, analyzed and annotated
443 clusters of putative orthologous genes for this group of viruses as well as an automatically generated version of
444 clusters of homologous genes for all NCLDV
445 (ftp://ftp.ncbi.nih.gov/pub/yutinn/Loki_Castle_NCLDV_2018/NCLDV_clusters/). Altogether, 8066 NCLDV
446 gene clusters were identified of which a substantial majority were family-specific. Nevertheless, almost 200
447 clusters were found to be shared between Pithoviridae and *Marseilleviridae* families (Figure 5). The numbers of
448 genes shared by each of these families with *Iridoviridae* were much smaller, conceivably, because of the small
449 genome size of iridoviruses that could have undergone reductive evolution (Figure 5). Conversely, there was
450 considerable overlap between the PIM group gene clusters and those of mimiviruses, presumably, due to the
451 large genome sizes of the mimiviruses, but potentially reflecting also substantial horizontal gene flow between
452 mimiviruses and pitho- and marseilleviruses (Figure 5). Only 13 genes comprised a genomic signature of the
453 PIM group, that is, genes that were shared by its three constituent families, to the exclusion of the rest of the
454 NCLDV.
455

456 To further explore the relationships between the gene repertoires of the PIM group and other NCLDV, we
457 constructed a neighbor-joining tree from the data on gene presence-absence
458 (ftp://ftp.ncbi.nih.gov/pub/yutinn/Loki_Castle_NCLDV_2018/NCLDV_clusters/). Notwithstanding the limited
459 gene sharing, the topology of the resulting tree (Figure 6) closely recapitulated the phylogenetic tree of the
460 conserved core genes (Figure 3). In particular, the PIM group appears as a clade in the gene presence-absence
461

462 tree albeit with a comparatively low support (Figure 6). Thus, despite the paucity of PIM-specific genes and the
463 substantial differences in the genome sizes between the three virus families, gene gain and loss processes within
464 the viral genetic core appear to track the evolution of the universally conserved genes.

465

466 The genomes of microbes and large viruses encompass many lineage-specific genes (often denoted ORFans)
467 that, in the course of evolution, are lost and gained by horizontal gene transfer at extremely high rates (99).
468 Therefore, the gene repertoire of a microbial or viral species (notwithstanding the well-known difficulties with
469 the species definition) or group is best characterized by the pangenome, i.e. the entirety of genes represented in
470 all isolates in the group (100-102). Most microbes have “open” pangenomes such that every sequenced genome
471 adds new genes to the pangenome (102, 103). The NCLDV pangenomes could be even wider open, judging
472 from the high percentage of ORFans, especially, in giant viruses (104). Examination of the PIM genes clusters
473 shows that 757 of the 1572 clusters (48%) were unique to the LCV, that is, had no detectable homologs in other
474 members of the group. Taking into account also the 4147 ORFans, the LCV represent the bulk of the PIM group
475 pangenome. Among the NCLDV clusters, 1100 of the 8066 (14%) are LCV-specific. Thus, notwithstanding the
476 limitations of the automated clustering procedure that could miss some distant similarities between proteins, the
477 discovery of the LCV substantially expands not only the pangenome of the PIM group but also the overall
478 NCLDV pangenome.

479

480 Annotation of the genes characteristic of (but not necessarily exclusive to) the PIM group reveals numerous,
481 highly diverse functions of either bacterial or eukaryotic provenance as suggested by the taxonomic affiliations
482 of homologs detected in database searches (Additional file 5). For example, a functional group of interest shared
483 by the three families in the PIM group include genes of apparent bacterial origin involved in various DNA
484 repair processes and nucleotide metabolism. The results of phylogenetic analysis of these genes are generally
485 compatible with bacterial origin although many branches are mixed, including also archaea and/or eukaryotes

486 and indicative of horizontal gene transfer (Figure 7). Notably, these trees illustrate the “hidden complexity” of
487 NCLDV evolution whereby homologous genes are independently captured by different groups of viruses. In the
488 trees for the two subunits of the SbcCD nuclease, the PIM group forms a clade but the homologs in mimiviruses
489 appear to be of distinct origin (Figure 7A,B) whereas in the trees for exonuclease V and dNMP kinase, the PMI
490 group itself splits between 3 branches (Figure 7C,D). The latter two trees also contain branches in which
491 different groups of the NCLDV, in particular, marseilleviruses and mimiviruses, are mixed, apparently
492 reflecting genes exchange between distinct viruses infecting the same host, such as amoeba.

493

494

495 **Loki’s Castle virophages**

496 Many members of the family *Mimiviridae* are associated with small satellite viruses that became known as
497 virophages (subsequently classified in the family *Lavidaviridae* (105-111). Two viophage-like sequences were
498 retrieved from Loki Castle metagenomes. According to the MCP phylogeny, they form a separate branch within
499 the Sputnik-like group (Figure 8A). This affiliation implies that these virophages are parasites of mimiviruses.
500 Both Loki’s Castle virophages encode the core viophage genes encoding the proteins involved in virion
501 morphogenesis, namely, MCP, minor capsid protein, packaging ATPase, and cysteine protease (Figure 8B and
502 Additional File 2 for protein annotations). Apart from these core genes, however, these virophages differ from
503 Sputnik. In particular, they lack the gene for the primase-helicase fusion protein that is characteristic of Sputnik
504 and its close relatives (112), but each encode a distinct helicase (Figure 8B).

505

506 **Putative promoter motifs in LCV and Loki’s Castle virophages**

507 To identify possible promoter sequences in the LCV genomes, we searched upstream regions of the predicted
508 LCV genes for recurring motifs using the MEME software (see Methods for details). In most of the bins, we
509 identified a conserved motif similar to the early promoters of poxviruses and mimiviruses (113) (AAAnTGA)

510 that is typically located within 40 to 20 nucleotides upstream of the predicted start codon (for the search results,
511 see: ftp://ftp.ncbi.nih.gov/pub/yutinn/Loki_Castle_NCLDV_2018/meme_motif_search/). To assess possible bin
512 contamination, we calculated frequencies of the conserved motifs per contig, for Marseillevirus-like and
513 Mimivirus-like bins. None of the contigs showed significantly reduced frequency of the conserved motif
514 (Additional file 7), supporting the virus origin of all the contigs.

515
516 Notably, the LCV virophage genomes also contain a conserved AT-rich motif upstream of each gene which is
517 likely to correspond to the late promoter of their hosts, similarly to the case of the Sputnik virophage that carries
518 late mimivirus promoters (114). However, the genomes of the two putative Klosneuviruses LCMiAC01 nor
519 LCMiAC02 that are represented among the LCV do not contain obvious counterparts to these predicted
520 virophage promoters (Additional file 8). Therefore, it appears most likely that the hosts of these virophages are
521 mimiviruses that are not represented in the LCV sequence set.

522
523 Of further interest is the detection of pronounced promoter-like motifs for pitho-like LCV (Additional file 9)
524 and irido-like LCV (Additional file 10). To our knowledge, no conserved promoter motifs have been so far
525 identified for these groups of viruses.

526
527
528 **Discussion**

529
530 Metagenomics has become the primary means of new virus discovery (51, 52, 115). Metagenomic sequence
531 analysis has greatly expanded many groups of viruses such that the viruses that have been identified earlier by
532 traditional methods have become isolated branches in the overall evolutionary trees in which most of the
533 diversity comes from metagenomic sequences (116-121). The analysis of the Loki's Castle metagenome

534 reported here has similarly expanded the Pithovirus branch of the NCLDV, and to a somewhat lesser extent, the
535 Marseillevirus branch. Although only one LCV genome, that of a Marseille-like virus, appears to be complete
536 and on a single contig, several other genomes seem to be near complete, and overall, the LCV genomic data are
537 sufficient to dramatically expand the pangenome of the PIM group, to add substantially to the NCLDV
538 pangenome as well, and to reveal notable evolutionary trends. One of such trends is the apparent independent
539 origin of giant viruses in more than one clade within both the Pithovirus and the Marseillevirus branches.
540 Although this observation should be interpreted with caution, given the lack of fully assembled LCV genomes,
541 it supports and extends the previous conclusions on the dynamic nature of NCLDV evolution (“genomic
542 accordion”) that led to the independent, convergent evolution of viral gigantism in several, perhaps, even all
543 NCLDV families (45, 48, 122, 123). Conversely, these findings are incompatible with the concept of reductive
544 evolution of NCLDV from giant viruses as the principal evolutionary mode. Another notable evolutionary trend
545 emerging from the LCV genome comparison is the apparent extensive gene exchange between Pitho-like and
546 Marseille-like viruses, and members of the *Mimiviridae*. Finally, it is important to note that the LCV analysis
547 reaffirms, on a greatly expanded dataset, the previously proposed monophyly of the PIM group of the NCLDV,
548 demonstrating robustness of the evolutionary analysis of conserved NCLDV genes (28, 45). Furthermore, a
549 congruent tree topology was obtained by gene content analysis, indicating that, despite the open pangenomes
550 and the dominance of unique genes, evolution of the genetic core of the NCLDV appears to track the sequence
551 divergence of the universal marker genes.

552

553 Like other giant viruses, several LCV encode multiple translation system components. Although none of
554 them rivals the near complete translation systems encoded by Klosneuviruses (46), Orpheovirus (19), and
555 especially, Tupanviruses (98), some are comparable, in this regard, to the Mimiviruses (45). The diverse origins
556 of the translation system components in LCV suggested by phylogenetic analysis are compatible with the

557 previous conclusions on the piecemeal capture of these genes by giant viruses as opposed to inheritance from a
558 common ancestor (43, 45).

559

560 The 23 NCLDV genome bins reconstructed in the present study only represent a small fraction of the full
561 NCLDV diversity as determined by DNA polymerase sequences present in marine sediments (Figure 1).
562 Notably, sequences closely matching the sequences in the NCLDV genome bins were identified only in the
563 Loki's Castle metagenomes, not in TARA oceans water column metagenomes or Earth Virome sequences.
564 Thus, the deep sea sediments represent a unique and unexplored habitat for NCLDVs. Further studies targeting
565 deep sea sediments will bring new insights into the diversity and genomic potential of these viruses.

566

567 Identification of the host range is one of the most difficult problems in metaviromics and also in the study of
568 giant viruses, even by traditional methods. Most of the giant viruses have been isolated by co-cultivation with
569 model amoeba species, and the natural hosts remains unknown. Notable exceptions are the giant viruses isolated
570 from marine flagellates *Cafeteria roenbergensis* (12) and *Bodo saltans* (35). The principal approach for
571 inferring the virus host range from metagenomics data is the analysis of co-occurrence of virus sequences with
572 those of potential hosts (124, 125). However, virtually no 18S rRNA gene sequences of eukaryotic origin were
573 detected in the Loki's Castle sediment samples, in a sharp contrast to the rich prokaryotic microbiota (61, 62).
574 The absence of potential eukaryotic hosts of the LCV strongly suggests that these viruses do not reproduce in
575 the sediments but rather could originate from virus particles that precipitate from different parts of the water
576 column. So far, however, closely related sequences have not been found in water column metagenomes (Figure
577 1). The eukaryotic hosts might have inhabited the shallower sediments, and although they have decomposed
578 over time, the resilient virus particles remain as a “fossil record”. Clearly, the hosts of these viruses remain to be
579 identified. An obvious and important limitation of this work – and any metagenomic study – is that the viruses
580 discovered here (we are now in a position to call the viruses without quotes, given the recent decisions of the

581 ICTV) have not been grown in a host culture. Accordingly, our understanding of their biology is limited to the
582 inferences made from the genomic sequence which, per force, cannot yield the complete picture. In the case of
583 the NCLDV, these limitations are exacerbated by the fact that their genomic DNA is not infectious, and
584 therefore, even the availability of the complete genome does not provide for growing the virus. The
585 metagenomic analyses must complement rather than replace traditional virology and newer culturomic
586 approaches.

587

588 Although the sediment samples used in this study have not been dated directly, determinations of
589 sedimentation rates in nearby areas show that these rates vary between 1-5 cm per 1000 years (126, 127). With
590 the fastest sedimentation rate considered, the sediments could be over 20,600 years old at the shallowest depth
591 (103 cm). Considering that *Pithovirus sibericum* and *Mollivirus sibericum* were revived from 30,000 year old
592 permafrost (17, 20), it might be possible to resuscitate some of the LCVs using similar methods. Isolation
593 experiments with giant viruses from deep sea sediments, now that we are aware of their presence, would be the
594 natural next step to learn more about their biology.

595

596 Regardless, the discovery of the LCV substantially expands the known ocean megavirome and demonstrates
597 the previously unsuspected high prevalence of Pitho-like viruses. Given that all this diversity comes from a
598 single site on the ocean floor, it appears clear that the megavirome is large and diverse, and metagenomics
599 analysis of NCLDV from other sites will bring many surprises.

600

601 Acknowledgements

602 We acknowledge the help from chief scientist R. B. Pedersen, the scientific party and the entire crew on board
603 the Norwegian research vessel G.O. Sars during the summer 2008, 2010 and 2014 expeditions. We thank the
604 Uppsala Multidisciplinary Center for Advanced Computational Science (UPPMAX) at Uppsala University and

605 the Swedish National Infrastructure for Computing (SNIC) at the PDC Center for High-Performance
606 Computing for providing computational resources. This work was supported by grants of the European
607 Research Council (ERC Starting grant 310039-PUZZLE_CELL), the Swedish Foundation for Strategic
608 Research (SSF-FFL5) and the Swedish Research Council (VR grant 2015-04959) to T.J.G.E.. N.Y., YIW, and
609 E.V.K. are funded through the Intramural Research program of the National Institutes of Health of the USA.
610

611

References

612

613

614

615

616

617

618

619

620

621

622

623

624

625

626

627

628

629

630

631

632

633

634

635

636

637

638

639

640

641

642

643

644

645

646

1. **Koonin EV, Yutin N.** 2010. Origin and evolution of eukaryotic large nucleo-cytoplasmic DNA viruses. *Intervirology*. **53**(5):284-292.
2. **Iyer LM, Aravind L, Koonin EV.** 2001. Common origin of four diverse families of large eukaryotic DNA viruses. *J Virol*. **75**(23):11720-11734.
3. **Iyer LM, Balaji S, Koonin EV, Aravind L.** 2006. Evolutionary genomics of nucleo-cytoplasmic large DNA viruses. *Virus Res*. **117**(1):156-184.
4. **La Scola B , et al.** 2003. A giant virus in amoebae. *Science*. **299**(5615):2033.
5. **Raoult D , et al.** 2004. The 1.2-megabase genome sequence of Mimivirus. *Science*. **306**(5700):1344-1350.
6. **Koonin EV.** 2005. Virology: Gulliver among the Lilliputians. *Curr Biol*. **15**(5):R167-169.
7. **Claverie JM , et al.** 2006. Mimivirus and the emerging concept of "giant" virus. *Virus Res*. **117**(1):133-144.
8. **Fischer MG.** 2016. Giant viruses come of age. *Curr Opin Microbiol*. **31**:50-57.
9. **Suzan-Monti M, La Scola B, Raoult D.** 2006. Genomic and evolutionary aspects of Mimivirus. *Virus Res*. **117**(1):145-155.
10. **Claverie JM, Abergel C, Ogata H.** 2009. Mimivirus. *Curr Top Microbiol Immunol*. **328**:89-121.
11. **Claverie JM , et al.** 2009. Mimivirus and Mimiviridae: giant viruses with an increasing number of potential hosts, including corals and sponges. *J Invertebr Pathol*. **101**(3):172-180.
12. **Fischer MG, Allen MJ, Wilson WH, Suttle CA.** 2010. Giant virus with a remarkable complement of genes infects marine zooplankton. *Proc Natl Acad Sci U S A*. **107**(45):19508-19513.
13. **Yutin N, Colson P, Raoult D, Koonin EV.** 2013. Mimiviridae: clusters of orthologous genes, reconstruction of gene repertoire evolution and proposed expansion of the giant virus family. *Virol J*. **10**:106.
14. **Philippe N , et al.** 2013. Pandoraviruses: amoeba viruses with genomes up to 2.5 Mb reaching that of parasitic eukaryotes. *Science*. **341**(6143):281-286.
15. **Yutin N, Koonin EV.** 2013. Pandoraviruses are highly derived phycodnaviruses. *Biol Direct*. **8**:25.
16. **Legendre M , et al.** 2018. Diversity and evolution of the emerging Pandoraviridae family. *Nat Commun*. **9**(1):2285.
17. **Legendre M , et al.** 2014. Thirty-thousand-year-old distant relative of giant icosahedral DNA viruses with a pandoravirus morphology. *Proc Natl Acad Sci U S A*. **111**(11):4274-4279.
18. **Andreani J , et al.** 2016. Cedratvirus, a Double-Cork Structured Giant Virus, is a Distant Relative of Pithoviruses. *Viruses*. **8**(11).
19. **Andreani J , et al.** 2017. Orpheovirus IHUMI-LCC2: A New Virus among the Giant Viruses. *Front Microbiol*. **8**:2643.

647 20. **Legendre M , et al.** 2015. In-depth study of Mollivirus sibericum, a new 30,000-y-old giant virus
648 infecting Acanthamoeba. *Proc Natl Acad Sci U S A.* **112**(38):E5327-5335.

649 21. **Boyer M , et al.** 2009. Giant Marseillevirus highlights the role of amoebae as a melting pot in
650 emergence of chimeric microorganisms. *Proc Natl Acad Sci U S A.* **106**(51):21848-21853.

651 22. **Colson P , et al.** 2013. "Marseilleviridae", a new family of giant viruses infecting amoebae. *Arch Virol.*
652 **158**(4):915-920.

653 23. **Reteno DG , et al.** 2015. Faustovirus, an asfarvirus-related new lineage of giant viruses infecting
654 amoebae. *J Virol.* **89**(13):6585-6594.

655 24. **Benamar S , et al.** 2016. Faustoviruses: Comparative Genomics of New Megavirales Family Members.
656 *Front Microbiol.* **7**:3.

657 25. **Abergel C, Legendre M, Claverie JM.** 2015. The rapidly expanding universe of giant viruses:
658 Mimivirus, Pandoravirus, Pithovirus and Mollivirus. *FEMS Microbiol Rev.* **39**(6):779-796.

659 26. **Colson P, de Lamballerie X, Fournous G, Raoult D.** 2012. Reclassification of giant viruses
660 composing a fourth domain of life in the new order Megavirales. *Intervirology.* **55**(5):321-332.

661 27. **Colson P , et al.** 2013. "Megavirales", a proposed new order for eukaryotic nucleocytoplasmic large
662 DNA viruses. *Arch Virol.* **158**(12):2517-2521.

663 28. **Yutin N, Wolf YI, Raoult D, Koonin EV.** 2009. Eukaryotic large nucleo-cytoplasmic DNA viruses:
664 clusters of orthologous genes and reconstruction of viral genome evolution. *Virol J.* **6**:223.

665 29. **Yutin N, Koonin EV.** 2012. Hidden evolutionary complexity of Nucleo-Cytoplasmic Large DNA
666 viruses of eukaryotes. *Virol J.* **9**:161.

667 30. **Boyer M, Gimenez G, Suzan-Monti M, Raoult D.** 2010. Classification and determination of possible
668 origins of ORFans through analysis of nucleocytoplasmic large DNA viruses. *Intervirology.* **53**(5):310-
669 320.

670 31. Moss B: **Poxviridae: the viruses and their replication.** In: *Fields Virology*. Edited by Fields BN,
671 Knipe DM, Howley PM, Griffin DE, vol. 2, 4th edn. Philadelphia: Lippincott, Williams & Wilkins;
672 2001: 2849-2884.

673 32. **Galindo I, Alonso C.** 2017. African Swine Fever Virus: A Review. *Viruses.* **9**(5).

674 33. **Suttle CA.** 2007. Marine viruses--major players in the global ecosystem. *Nat Rev Microbiol.* **5**(10):801-
675 812.

676 34. **Rohwer F, Thurber RV.** 2009. Viruses manipulate the marine environment. *Nature.* **459**(7244):207-
677 212.

678 35. **Deeg CM, Chow CT, Suttle CA.** 2018. The kinetoplastid-infecting *Bodo saltans* virus (BsV), a window
679 into the most abundant giant viruses in the sea. *Elife.* **7**.

680 36. **Claverie JM.** 2006. Viruses take center stage in cellular evolution. *Genome Biol.* **7**(6):110.

681 37. **Colson P, Gimenez G, Boyer M, Fournous G, Raoult D.** 2011. The giant *Cafeteria roenbergensis*
682 virus that infects a widespread marine phagocytic protist is a new member of the fourth domain of Life.
683 *PLoS One.* **6**(4):e18935.

684 38. **Legendre M, Arslan D, Abergel C, Claverie JM.** 2012. Genomics of Megavirus and the elusive fourth
685 domain of Life. *Commun Integr Biol.* **5**(1):102-106.

686 39. **Nasir A, Kim KM, Caetano-Anolles G.** 2012. Giant viruses coexisted with the cellular ancestors and
687 represent a distinct supergroup along with superkingdoms Archaea, Bacteria and Eukarya. *BMC Evol
688 Biol.* **12**:156.

689 40. **Nasir A, Kim KM, Caetano-Anolles G.** 2017. Phylogenetic Tracings of Proteome Size Support the
690 Gradual Accretion of Protein Structural Domains and the Early Origin of Viruses from Primordial Cells.
691 *Front Microbiol.* **8**:1178.

692 41. **Lopez-Garcia P.** 2012. The place of viruses in biology in light of the metabolism- versus-replication-
693 first debate. *Hist Philos Life Sci.* **34**(3):391-406.

694 42. **Forterre P, Krupovic M, Prangishvili D.** 2014. Cellular domains and viral lineages. *Trends Microbiol.*
695 **22**(10):554-558.

696 43. **Moreira D, Brochier-Armanet C.** 2008. Giant viruses, giant chimeras: the multiple evolutionary
697 histories of Mimivirus genes. *BMC Evol Biol.* **8**:12.

698 44. **Williams TA, Embley TM, Heinz E.** 2011. Informational gene phylogenies do not support a fourth
699 domain of life for nucleocytoplasmic large DNA viruses. *PLoS One.* **6**(6):e21080.

700 45. **Yutin N, Wolf YI, Koonin EV.** 2014. Origin of giant viruses from smaller DNA viruses not from a
701 fourth domain of cellular life. *Virology.*

702 46. **Schulz F , et al.** 2017. Giant viruses with an expanded complement of translation system components.
703 *Science.* **356**(6333):82-85.

704 47. **Elde NC , et al.** 2012. Poxviruses deploy genomic accordions to adapt rapidly against host antiviral
705 defenses. *Cell.* **150**(4):831-841.

706 48. **Filee J.** 2013. Route of NCLDV evolution: the genomic accordion. *Curr Opin Virol.* **3**(5):595-599.

707 49. **Filee J, Pouget N, Chandler M.** 2008. Phylogenetic evidence for extensive lateral acquisition of
708 cellular genes by Nucleocytoplasmic large DNA viruses. *BMC Evol Biol.* **8**:320.

709 50. **Filee J, Chandler M.** 2010. Gene exchange and the origin of giant viruses. *Intervirology.* **53**(5):354-
710 361.

711 51. **Simmonds P , et al.** 2017. Consensus statement: Virus taxonomy in the age of metagenomics. *Nat Rev
712 Microbiol.* **15**(3):161-168.

713 52. **Zhang YZ, Shi M, Holmes EC.** 2018. Using Metagenomics to Characterize an Expanding Virosphere.
714 *Cell.* **172**(6):1168-1172.

715 53. **Koonin EV, Dolja VV.** 2018. Metaviromics: a tectonic shift in understanding virus evolution. *Virus
716 Res.* **246**:A1-A3.

717 54. **Pagnier I , et al.** 2013. A decade of improvements in Mimiviridae and Marseilleviridae isolation from
718 amoeba. *Intervirology*. **56**(6):354-363.

719 55. **Khalil JY , et al.** 2016. High-Throughput Isolation of Giant Viruses in Liquid Medium Using
720 Automated Flow Cytometry and Fluorescence Staining. *Front Microbiol*. **7**:26.

721 56. **Halary S, Temmam S, Raoult D, Desnues C.** 2016. Viral metagenomics: are we missing the giants?
722 *Curr Opin Microbiol*. **31**:34-43.

723 57. **Paez-Espino D , et al.** 2016. Uncovering Earth's virome. *Nature*. **536**(7617):425-430.

724 58. **Verneau J, Levasseur A, Raoult D, La Scola B, Colson P.** 2016. MG-Digger: An Automated Pipeline
725 to Search for Giant Virus-Related Sequences in Metagenomes. *Front Microbiol*. **7**:428.

726 59. **Brown CT , et al.** 2015. Unusual biology across a group comprising more than 15% of domain
727 Bacteria. *Nature*. **523**(7559):208-211.

728 60. **Spang A, Caceres EF, Ettema TJG.** 2017. Genomic exploration of the diversity, ecology, and
729 evolution of the archaeal domain of life. *Science*. **357**(6351).

730 61. **Spang A , et al.** 2015. Complex archaea that bridge the gap between prokaryotes and eukaryotes.
731 *Nature*. **521**(7551):173-179.

732 62. **Zaremba-Niedzwiedzka K , et al.** 2017. Asgard archaea illuminate the origin of eukaryotic cellular
733 complexity. *Nature*. **541**(7637):353-358.

734 63. **Jorgensen SL , et al.** 2012. Correlating microbial community profiles with geochemical data in highly
735 stratified sediments from the Arctic Mid-Ocean Ridge. *Proc Natl Acad Sci U S A*. **109**(42):E2846-2855.

736 64. **Jorgensen SL, Thorseth IH, Pedersen RB, Baumberger T, Schleper C.** 2013. Quantitative and
737 phylogenetic study of the Deep Sea Archaeal Group in sediments of the Arctic mid-ocean spreading
738 ridge. *Front Microbiol*. **4**:299.

739 65. **Hyatt D , et al.** 2010. Prodigal: prokaryotic gene recognition and translation initiation site identification.
740 *BMC Bioinformatics*. **11**:119.

741 66. **Camacho C , et al.** 2009. BLAST+: architecture and applications. *BMC Bioinformatics*. **10**:421.

742 67. **Katoh K, Standley DM.** 2013. MAFFT multiple sequence alignment software version 7: improvements
743 in performance and usability. *Mol Biol Evol*. **30**(4):772-780.

744 68. **Waterhouse AM, Procter JB, Martin DM, Clamp M, Barton GJ.** 2009. Jalview Version 2--a
745 multiple sequence alignment editor and analysis workbench. *Bioinformatics*. **25**(9):1189-1191.

746 69. **Capella-Gutierrez S, Silla-Martinez JM, Gabaldon T.** 2009. trimAl: a tool for automated alignment
747 trimming in large-scale phylogenetic analyses. *Bioinformatics*. **25**(15):1972-1973.

748 70. **Nguyen LT, Schmidt HA, von Haeseler A, Minh BQ.** 2015. IQ-TREE: a fast and effective stochastic
749 algorithm for estimating maximum-likelihood phylogenies. *Mol Biol Evol*. **32**(1):268-274.

750 71. **Hoang DT, Chernomor O, von Haeseler A, Minh BQ, Vinh LS.** 2018. UFBoot2: Improving the
751 Ultrafast Bootstrap Approximation. *Mol Biol Evol*. **35**(2):518-522.

752 72. **Kalyaanamoorthy S, Minh BQ, Wong TKF, von Haeseler A, Jermiin LS.** 2017. ModelFinder: fast
753 model selection for accurate phylogenetic estimates. *Nat Methods.* **14**(6):587-589.

754 73. **Dick GJ , et al.** 2009. Community-wide analysis of microbial genome sequence signatures. *Genome*
755 *Biol.* **10**(8):R85.

756 74. **Bray NL, Pimentel H, Melsted P, Pachter L.** 2016. Near-optimal probabilistic RNA-seq
757 quantification. *Nat Biotechnol.* **34**(5):525-527.

758 75. **Alneberg J , et al.** 2014. Binning metagenomic contigs by coverage and composition. *Nat Methods.*
759 **11**(11):1144-1146.

760 76. **Karst SM, Kirkegaard RH, Albertsen M.** 2016. Mmgenome: a toolbox for reproducible genome
761 extraction from metagenomes. *bioRxiv* **059121**.

762 77. **Bankevich A , et al.** 2012. SPAdes: a new genome assembly algorithm and its applications to single-
763 cell sequencing. *J Comput Biol.* **19**(5):455-477.

764 78. **Ounit R, Wanamaker S, Close TJ, Lonardi S.** 2015. CLARK: fast and accurate classification of
765 metagenomic and genomic sequences using discriminative k-mers. *BMC Genomics.* **16**:236.

766 79. **Gurevich A, Saveliev V, Vyahhi N, Tesler G.** 2013. QUAST: quality assessment tool for genome
767 assemblies. *Bioinformatics.* **29**(8):1072-1075.

768 80. **Seemann T.** 2013. Ten recommendations for creating usable bioinformatics command line software.
769 *Gigascience.* **2**(1):15.

770 81. **Langmead B, Salzberg SL.** 2012. Fast gapped-read alignment with Bowtie 2. *Nat Methods.* **9**(4):357-
771 359.

772 82. **Li H, Durbin R.** 2009. Fast and accurate short read alignment with Burrows-Wheeler transform.
773 *Bioinformatics.* **25**(14):1754-1760.

774 83. **Buchfink B, Xie C, Huson DH.** 2015. Fast and sensitive protein alignment using DIAMOND. *Nat*
775 *Methods.* **12**(1):59-60.

776 84. **Kurtz S , et al.** 2004. Versatile and open software for comparing large genomes. *Genome Biol.*
777 **5**(2):R12.

778 85. **Sunagawa S , et al.** 2015. Ocean plankton. Structure and function of the global ocean microbiome.
779 *Science.* **348**(6237):1261359.

780 86. **Zhu W, Lomsadze A, Borodovsky M.** 2010. Ab initio gene identification in metagenomic sequences.
781 *Nucleic Acids Res.* **38**(12):e132.

782 87. **Lowe TM, Chan PP.** 2016. tRNAscan-SE On-line: integrating search and context for analysis of
783 transfer RNA genes. *Nucleic Acids Res.* **44**(W1):W54-57.

784 88. **Edgar RC.** 2004. MUSCLE: multiple sequence alignment with high accuracy and high throughput.
785 *Nucleic Acids Res.* **32**(5):1792-1797.

786 89. **Yutin N, Makarova KS, Mekhedov SL, Wolf YI, Koonin EV.** 2008. The deep archaeal roots of
787 eukaryotes. *Mol Biol Evol.* **25**(8):1619-1630.

788 90. **Price MN, Dehal PS, Arkin AP.** 2010. FastTree 2--approximately maximum-likelihood trees for large
789 alignments. *PLoS ONE*. **5**(3):e9490.

790 91. **Guindon S, Gascuel O.** 2003. A simple, fast, and accurate algorithm to estimate large phylogenies by
791 maximum likelihood. *Syst Biol*. **52**(5):696-704.

792 92. **Edgar RC.** 2010. Search and clustering orders of magnitude faster than BLAST. *Bioinformatics*.
793 **26**(19):2460-2461.

794 93. **Soding J.** 2005. Protein homology detection by HMM-HMM comparison. *Bioinformatics*. **21**(7):951-
795 960.

796 94. **Altschul SF , et al.** 1997. Gapped BLAST and PSI-BLAST: a new generation of protein database search
797 programs. *Nucleic Acids Res*. **25**(17):3389-3402.

798 95. **Saitou N, Nei M.** 1987. The neighbor-joining method: a new method for reconstructing phylogenetic
799 trees. *Mol Biol Evol*. **4**(4):406-425.

800 96. **Bailey TL , et al.** 2009. MEME SUITE: tools for motif discovery and searching. *Nucleic Acids Res*.
801 **37**(Web Server issue):W202-208.

802 97. **Crooks GE, Hon G, Chandonia JM, Brenner SE.** 2004. WebLogo: a sequence logo generator.
803 *Genome Res*. **14**(6):1188-1190.

804 98. **Abrahao J , et al.** 2018. Tailed giant Tupanvirus possesses the most complete translational apparatus of
805 the known virosphere. *Nat Commun*. **9**(1):749.

806 99. **Wolf YI, Makarova KS, Lobkovsky AE, Koonin EV.** 2016. Two fundamentally different classes of
807 microbial genes. *Nat Microbiol*. **2**:16208.

808 100. **Medini D, Donati C, Tettelin H, Msignani V, Rappuoli R.** 2005. The microbial pan-genome. *Curr
809 Opin Genet Dev*. **15**(6):589-594.

810 101. **Tettelin H, Riley D, Cattuto C, Medini D.** 2008. Comparative genomics: the bacterial pan-genome.
811 *Curr Opin Microbiol*. **11**(5):472-477.

812 102. **Vernikos G, Medini D, Riley DR, Tettelin H.** 2015. Ten years of pan-genome analyses. *Curr Opin
813 Microbiol*. **23**:148-154.

814 103. **Puigbo P, Lobkovsky AE, Kristensen DM, Wolf YI, Koonin EV.** 2014. Genomes in turmoil:
815 quantification of genome dynamics in prokaryote supergenomes. *BMC Biol*. **12**:66.

816 104. **Aherfi S , et al.** 2018. A Large Open Pangenome and a Small Core Genome for Giant Pandoraviruses.
817 *Front Microbiol*. **9**:1486.

818 105. **La Scola B , et al.** 2008. The virophage as a unique parasite of the giant mimivirus. *Nature*.
819 **455**(7209):100-104.

820 106. **Fischer MG, Suttle CA.** 2011. A virophage at the origin of large DNA transposons. *Science*.
821 **332**(6026):231-234.

822 107. **Zhou J , et al.** 2015. Three novel virophage genomes discovered from Yellowstone Lake metagenomes.
823 *J Virol*. **89**(2):1278-1285.

824 108. **Oh S, Yoo D, Liu WT.** 2016. Metagenomics Reveals a Novel Virophage Population in a Tibetan
825 Mountain Lake. *Microbes Environ.* **31**(2):173-177.

826 109. **Yutin N, Kapitonov VV, Koonin EV.** 2015. A new family of hybrid virophages from an animal gut
827 metagenome. *Biol Direct.* **10**:19.

828 110. **Yutin N, Raoult D, Koonin EV.** 2013. Virophages, polintons, and transpovirons: a complex
829 evolutionary network of diverse selfish genetic elements with different reproduction strategies. *Virol J.*
830 **10**:158.

831 111. **Krupovic M, Kuhn JH, Fischer MG.** 2016. A classification system for virophages and satellite
832 viruses. *Arch Virol.* **161**(1):233-247.

833 112. **Iyer LM, Abhiman S, Aravind L.** 2008. A new family of polymerases related to superfamily A DNA
834 polymerases and T7-like DNA-dependent RNA polymerases. *Biol Direct.* **3**:39.

835 113. **Oliveira GP , et al.** 2017. Promoter Motifs in NCLDV: An Evolutionary Perspective. *Viruses.* **9**(1).

836 114. **Legendre M , et al.** 2010. mRNA deep sequencing reveals 75 new genes and a complex transcriptional
837 landscape in Mimivirus. *Genome Res.* **20**(5):664-674.

838 115. **Simmonds P.** 2015. Methods for virus classification and the challenge of incorporating metagenomic
839 sequence data. *J Gen Virol.* **96**(Pt 6):1193-1206.

840 116. **Shi M , et al.** 2016. Redefining the invertebrate RNA virosphere. *Nature.*

841 117. **Shi M , et al.** 2018. The evolutionary history of vertebrate RNA viruses. *Nature.* **556**(7700):197-202.

842 118. **Shi M, Zhang YZ, Holmes EC.** 2018. Meta-transcriptomics and the evolutionary biology of RNA
843 viruses. *Virus Res.* **243**:83-90.

844 119. **Dolja VV, Koonin EV.** 2018. Metagenomics reshapes the concepts of RNA virus evolution by
845 revealing extensive horizontal virus transfer. *Virus Res.* **244**:36-52.

846 120. **Yutin N , et al.** 2018. Discovery of an expansive bacteriophage family that includes the most abundant
847 viruses from the human gut. *Nat Microbiol.* **3**(1):38-46.

848 121. **Yutin N, Backstrom D, Ettema TJG, Krupovic M, Koonin EV.** 2018. Vast diversity of prokaryotic
849 virus genomes encoding double jelly-roll major capsid proteins uncovered by genomic and metagenomic
850 sequence analysis. *Virol J.* **15**(1):67.

851 122. **Rodrigues RAL, Abrahao JS, Drumond BP, Kroon EG.** 2016. Giants among larges: how gigantism
852 impacts giant virus entry into amoebae. *Curr Opin Microbiol.* **31**:88-93.

853 123. **Koonin EV, Yutin N.** 2018. Evolution of the Large Nucleocytoplasmic DNA Viruses of eukaryotes and
854 convergent origins of viral gigantism. *Advances Virus Research.* **in press**.

855 124. **Edwards RA, McNair K, Faust K, Raes J, Dutilh BE.** 2016. Computational approaches to predict
856 bacteriophage-host relationships. *FEMS Microbiol Rev.* **40**(2):258-272.

857 125. **Coutinho FH , et al.** 2017. Marine viruses discovered via metagenomics shed light on viral strategies
858 throughout the oceans. *Nat Commun.* **8**:15955.

859 126. **Bauch HA , et al.** 2001. A multiproxy reconstruction of the evolution of deep and surface waters in the
860 subarctic Nordic seas over the last 30,000 yr. *Quaternary Science Reviews*. **20**(4):659-678.

861 127. **Haflidason H, De Alvaro MM, Nygard A, Sejrup H, P., Laberg JS.** 2007. Holocene sedimentary
862 processes in the Andøya Canyon system, north Norway. *Marine Geology*. **246**(2-4):86-104.

863 128. **Roux S , et al.** 2017. Ecogenomics of virophages and their giant virus hosts assessed through time series
864 metagenomics. *Nat Commun*. **8**(1):858.

865

866

867 **Figure legends**

868
869
870

871 **Figure 1. Diversity of the NCLDV DNAP sequences in the Loki's Castle sediment metagenomes**
872 **(orange), and the TARA oceans (turquoise), and EarthVirome (purple) databases.** Reference sequences
873 are shown in black. The binned NCLDV genomes are marked with a star. Branches with bootstrap values above
874 95 are marked with a black circle. The maximum likelihood phylogeny was constructed as described under
875 Methods.

876

877 **Figure 2. Flowchart of the metagenomic binning procedures.** Two main binning approaches were used:
878 differential coverage binning (DC), and co-assembly binning (CA). DC: Reads from four different samples
879 were assembled into four metagenomes. The metagenomes were screened for NCLDV DNAP, and contigs were
880 binned with CONCOCT and ESOM. The raw CONCOCT and ESOM bins were combined and refined using
881 Mmgenome. The refined bins were put through taxonomic filtering, keeping only the contigs encoding at least
882 one NCLDV gene, and finally, reassembled. CA: A database containing the refined DC bins and NCLDV
883 reference genomes was used to create profiles to extract reads from the metagenomes. The reads were combined
884 and co-assembled. This step was followed by CONCOCT binning, Mmgenome bin refinement and taxonomic
885 filtering. Finally, the DC bins and CA bins were annotated and the best bins were chosen by comparing
886 sequence statistics, completeness and redundancy of marker genes, and marker gene phylogenies (see
887 Additional File 1 for details).

888

889 **Figure 3. Phylogenetic tree of three concatenated, universally conserved NCLDV proteins: DNA**
890 **polymerase, major capsid protein, and A18-like helicase.** Support values were obtained using 100 bootstrap
891 replications; branches with support less than 50% were collapsed. Scale bars represent the number of amino

892 acid (aa) substitutions per site. The inset shows the *Mimiviridae* branch. Triangles show collapsed branches.
893 The LCV sequences are color-coded as follows: red, Pitho-like; green, Marseille-like (a deep branch shown in
894 dark green); orange, Irido-like; blue, Mimi (Klosneu)-like.

895
896

Figure 4. Phylogenies of selected translation system components encoded by Loki's Castle viruses.

897 A, translation initiation factor eIF2b
898 B, aspartyl/asparaginyl-tRNA synthetase, AsnS
899 C, tyrosyl-tRNA synthetase, TyrS,
900 D, methionyl-tRNA synthetase, MetS. All branches are color-coded according to taxonomic affinity (see
901 Additional File 3 for the full trees). The numbers at the internal branches indicate local likelihood-based support
902 (percentage points).

903
904

Figure 5. Shared and unique genes in four NCLDV families that include Loki's Castle viruses. The
905 numbers correspond to NCLDV clusters that contain at least one protein from Mimi-, Marseille-, Pitho, and -
906 Iridoviridae, but are absent from other NCLDV families.

907
908

Figure 6. Gene presence-absence tree of the NCLDV including the Loki's Castle viruses. The Neighbor-
909 Joining dendrogram was reconstructed from the matrix of pairwise distances calculated from binary phyletic
910 patterns of the NCLDV clusters. The numbers at internal branches indicate bootstrap support (percentage
911 points); numbers below 50% are not shown.

912
913

Figure 7. Phylogenies of selected repair and nucleotide metabolism genes of the Pitho-Irido-Marseille
914 **virus group including Loki's Castle viruses.**

915 A, SbcCD nuclease, ATPase subunit SbcC

916 B, SbcCD nuclease, nuclease subunit SbcD
917 C, exonuclease V;
918 D, dNMP kinase.

919 The numbers at the internal branches indicate local likelihood-based support (percentage points). Genbank
920 protein IDs, wherever available, are shown after ‘@’. Taxa abbreviations are as follows: A DP, Archaea;
921 DPANN group; A TA, Thaumarchaeota; A Ea, Euryarchaeota; B FC, Bacteroidetes; B Fu, Fusobacteria; B Pr,
922 Proteobacteria; B Te, Firmicutes; B un, unclassified Bacteria; E Op, Opisthokonta; N Pi, ”Pithoviridae”; N Ac,
923 Ascoviridae; N As, Asfarviridae; N Ma, Marseilleviridae; N Mi, Mimiviridae; N Pa, Pandoraviridae; N Ph,
924 Phycodnaviridae; V ds, double-strand DNA viruses.

925
926 **Figure 8. Loki’s Castle virophages.**

927 A, Phylogenetic tree of virophage major capsid proteins. Reference virophages from GenBank are marked with
928 black font (the three prototype virophages are shown in bold), environmental virophages shown in blue (128)
929 and green (wgs portion of GenBank).
930 B, Genome maps of Loki’s Castle virophages compared with Sputnik virophage. Green and blue triangles mark
931 direct and inverted repeats. Pentagons with a thick outline represent conserved virophage genes.
932

933 **Additional files**
934 Additional File 1 – Supplementary binning methods and figures
935 Additional File 2 – LCV and LC virophage protein annotation
936 Additional File 3 – DNAP, MCP, A18hel, and translation protein trees
937 Additional File 4. – virophage genome maps
938 Additional File 5. – taxonomic breakdown of psi-BLAST hits retrieved with profiles created from selected
939 PIM clusters (clusters of four or more proteins, less conserved NCLDV genes).
940 Additional File 6. – Repeats plots
941 Additional File 7. – Conserved promoter-like motif frequencies in selected LCV bins
942 Additional File 8. – Conserved promoter-like motifs in the LCMiAC01 and LCMiAC02 bins, and LCV
943 virophages
944 Additonal File 9. - Conserved promoter-like motifs in pitho-like LCV.
945 Additonal File 10. - Conserved promoter-like motifs in Marseille-like and irido-like LCV.
946
947
948 More supplementary material:
949 ftp://ftp.ncbi.nih.gov/pub/yutinn/Loki_Castle_NCLDV_2018/
950
951
952
953
954
955
956
957
958
959
960

961
962
963
964
965
966
967
968
969
970
971
972
973
974
975
976
977
978
979
980
981
982

Table 1. The 23 NCLDV bins from Loki's Castle.

bin/virus		# of contigs	min contig length, nt	max contig length, nt	total contig length, nt	# of predicted proteins	MCP ^a	DNAp	ATP	RNApA	RNApB	D5hel	A18hel	VLTF3	VLTF2	RNAp5	Erv1	RNAlig	TopoII	FLAP	TFIIB
LCPAC001	Pitho-like	12	8088	60499	249064	227	1	1	0	1	1	0	1	0	0	0	2	1	1	0	0
LCPAC101	Pitho-like	26	6043	46492	466072	373	1	1	0	1	1	1	1	0	1	1	0	1	1	1	1
LCPAC102	Pitho-like	12	6510	44810	285593	229	1	1	0	1	1	0	0	0	1	0	3	1	0	1	1
LCPAC103	Pitho-like	17	5380	23680	204602	186	1	1	0	1	1	1	1	1	1	1	0	1	1	0	1
LCPAC104	Pitho-like	4	6208	129049	218903	194	1	1	0	1	1	1	1	1	1	1	1	1	1	1	1
LCPAC201	Pitho-like	11	5186	168698	428611	327	1	1	0	1	2	1	1	1	1	1	1	1	1	1	1
LCPAC202	Pitho-like	26	5141	72684	443964	354	1	2	0	1	2	1	1	1	1	1	1	1	1	1	0
LCPAC302	Pitho-like	30	5274	20428	290561	294	0	1	0	1	1	0	0	1	1	1	1	0	1	0	0
LCPAC304	Pitho-like	12	11737	173767	638759	688	1	1	0	1	1	1	1	1	1	1	0	1	1	1	1
LCPAC401	Pitho-like	11	7155	114453	484752	504	1	1	0	1	1	1	1	1	1	2	1	0	1	1	1
LCPAC403	Pitho-like	6	24087	117884	420388	430	1	1	0	1	1	1	1	1	1	2	0	1	1	1	1
LCPAC404	Pitho-like	10	11211	84762	436585	390	1	1	0	1	1	1	1	1	1	2	0	1	1	1	1
LCPAC406	Pitho-like	10	11113	75955	384297	401	1	1	0	1	1	1	1	1	1	2	1	0	1	1	1
LCDPAC01	Pitho-like	21	5383	31931	282320	282	1	1	0	1	1	1	1	1	1	0	1	0	1	1	0
LCDPAC02	Pitho-like	9	6786	90916	367310	390	1	1	0	1	1	1	1	0	0	1	1	0	1	0	0
LCMAC101	Marseille-like	7	15190	393561	763048	793	1	1	1	1	1	1	1	1	1	1	1	1	1	1	1
LCMAC102	Marseille-like	1	395459	395459	395459	465	1	1	1	1	1	1	1	1	1	1	1	1	1	1	1
LCMAC103	Marseille-like	9	14346	69824	389984	427	1	1	1	1	1	1	1	1	0	1	0	1	1	1	0
LCMAC201	Marseille-like	25	6728	57873	565697	566	1	1	1	1	1	0	1	1	0	1	2	1	1	1	1
LCMAC202	Marseille-like	19	6906	153726	705352	672	1	1	2	1	1	1	1	1	0	1	2	1	1	1	1
LCIVAC01	Iridovirus-like	19	5375	17223	198495	222	0	1	0	1	1	1	1	0	1	0	1	1	1	0	1
LCMiAC01	Mimivirus-like	18	8458	85120	672112	571	6	1	1	1	1	1	1	1	1	1	1	1	1	1	0
LCMiAC02	Mimivirus-like	21	8237	131456	642939	583	6	1	2	1	1	2	1	2	1	1	1	1	1	1	1
Cedratvirus A11			589068	574	574	1	1	0	1	1	1	1	1	1	1	1	1	1	1	1	1
Orpheovirus IHUMI LCC2			1473573	1199	1199	1	1	0	1	1	1	1	1	1	1	1	1	1	1	1	1
Pithovirus sibericum			610033	425	425	1	1	0	1	1	1	1	1	1	1	1	1	1	1	1	1
Marseillevirus			369360	403	403	1	1	1	1	1	1	1	1	1	1	1	1	1	1	1	1
Diadromus pulchellus ascovirus 4a			119343	119	119	1	1	1	1	1	1	1	0	1	1	1	1	1	0	0	1
Heliothis virescens ascovirus 3e			186262	180	180	1	1	1	1	1	1	1	0	1	1	1	1	1	0	1	1
Lymphocystis disease virus			186250	239	239	1	1	1	1	1	1	1	1	1	1	1	1	1	1	0	1
Frog virus 3			105903	99	99	1	1	1	1	1	1	1	0	1	1	1	1	1	0	1	0
Wiseana iridescent virus			205791	193	193	1	1	1	1	1	1	1	1	1	1	1	1	1	1	1	1
Cafeteria roenbergensis virus BV PW1			617453	544	544	3	1	1	1	1	1	1	1	1	0	1	1	0	1	1	1
Acanthamoeba polyphaga mimivirus			1181549	979	979	4	1	2	1	1	1	1	1	1	1	1	1	0	1	1	1
Klosneuvirus KNV1			1573084	1545	1545	7	1	3	1	1	1	2	1	1	1	1	3	2	1	2	1

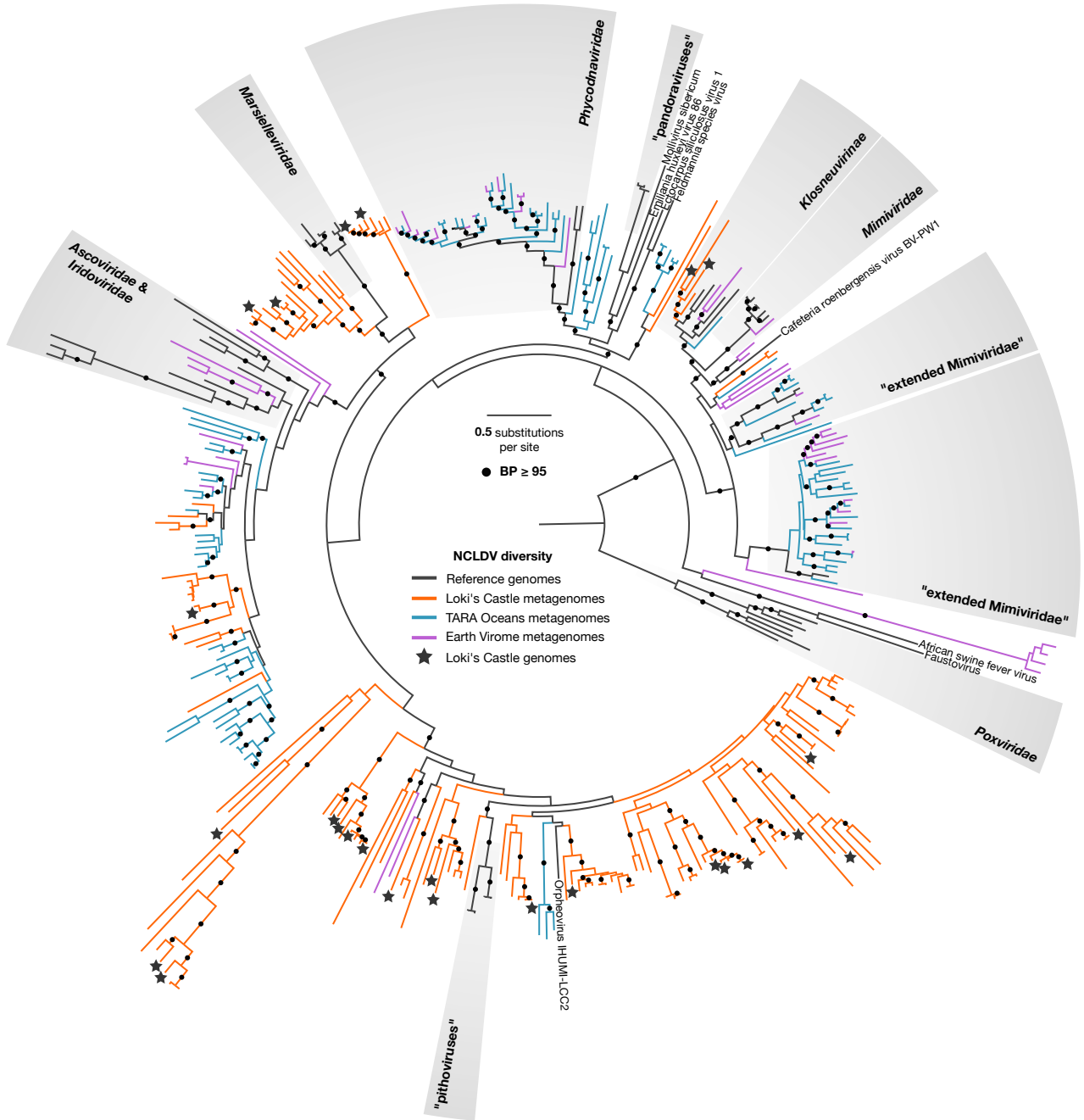
^{a)} MCP, NCLDV major capsid protein (NCVOG0022); DNAP, DNA polymerase family B, elongation subunit (NCVOG0038); ATP, A32-like packaging ATPase (NCVOG0249); RNAPA, DNA-directed RNA polymerase subunit alpha (NCVOG0274); RNAPB, DNA-directed RNA polymerase subunit beta (NCVOG0271); D5hel, D5-like helicase-primase (NCVOG0023); A18hel, A18-like helicase (NCVOG0076); VLTF3, Poxvirus Late Transcription Factor VLTF3 (NCVOG0262); VLTF2, A1L transcription factor/late TF VLTF-2 (NCVOG1164); RNAP5, DNA-directed RNA polymerase subunit 5 (NCVOG0273); Erv1, Erv1/Alr family disulfide (thiol) oxidoreductase (NCVOG0052); RNAlig, RNA ligase (NCVOG1088); TopoII, DNA topoisomerase II (NCVOG0037); FLAP, Flap endonuclease (NCVOG1060); TFIIB, transcription initiation factor IIB (NCVOG1127).

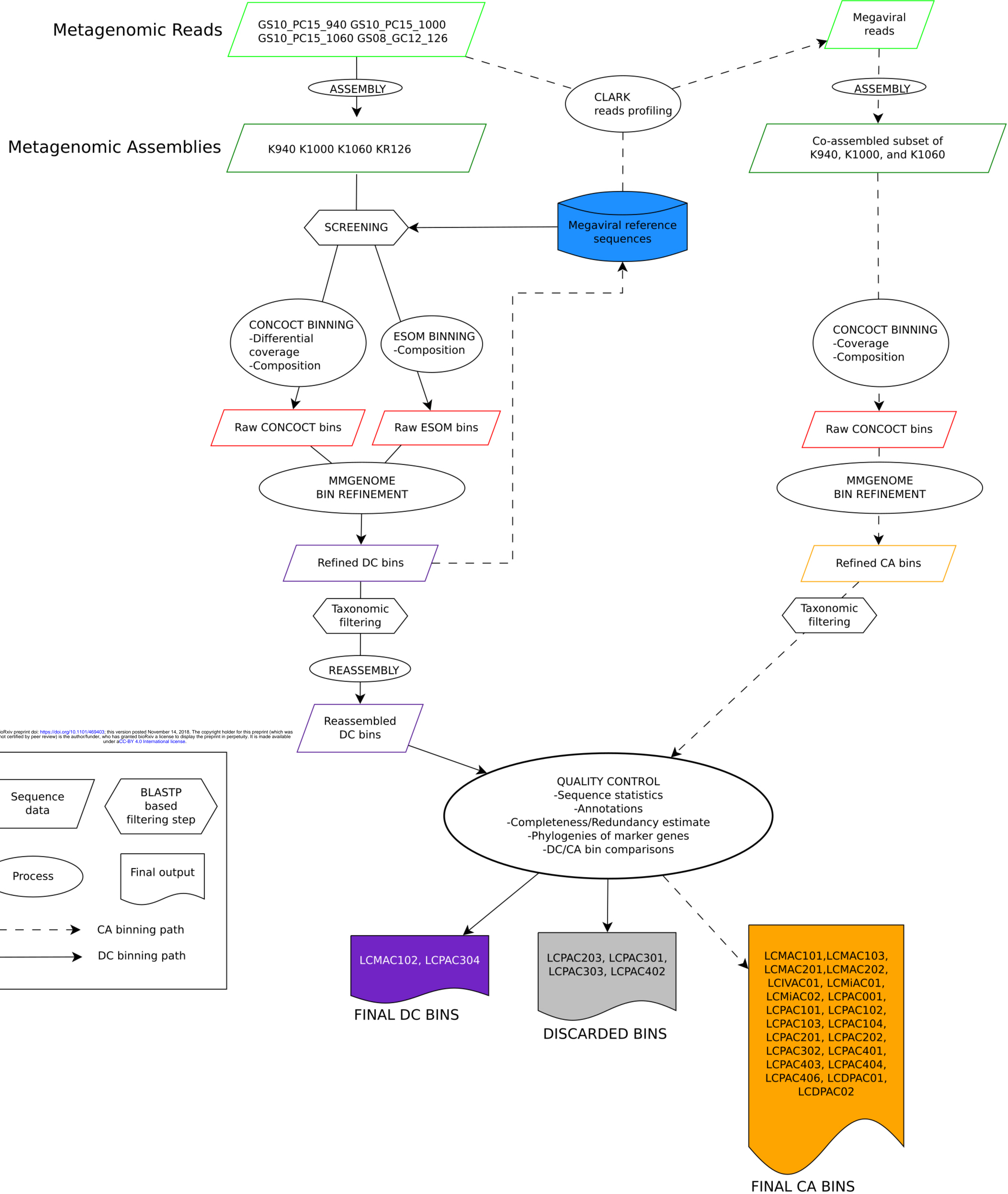
bioRxiv preprint doi: <https://doi.org/10.1101/469103>; this version posted March 20, 2016. The copyright holder for this preprint (which was not certified by peer review) is the author/funder, who has granted bioRxiv a license to display the preprint in perpetuity. It is made available under aCC-BY 4.0 International license.

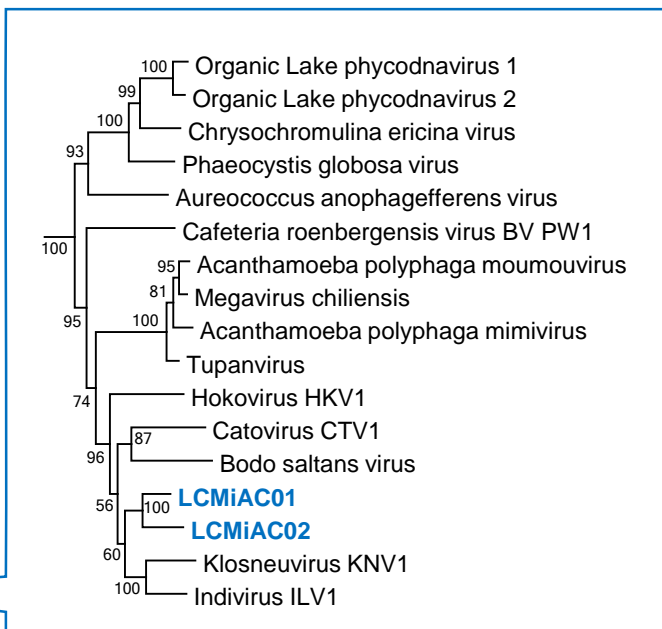
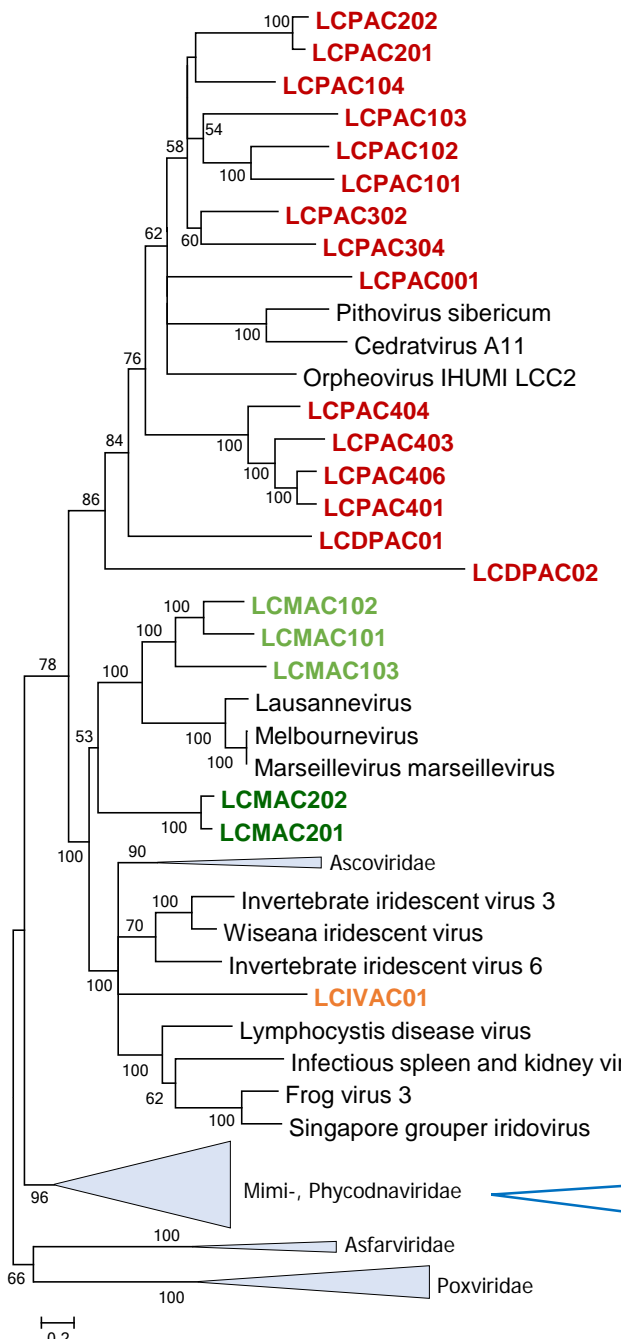
	AlaS	AsnS	AspS	GlnS	HisS	IleS	LeuS	MetS	ProS	Pth2	RLI1	ThrS	TrpS	TyrS	eiF1	eiF1a	eiF2a	eiF2b	eiF2g	eiF4e	eiF5b	eRF1	tRNA
LCPAC001	1							1															5
LCPAC101			1																				2
LCPAC102																							3
LCPAC103																							
LCPAC104																							4
LCPAC201																							
LCPAC202																							
LCPAC302												1											
LCPAC304	1										1	1	1					1					21
LCPAC401																							
LCPAC403																							
LCPAC404																			1				
LCPAC406																							
LCDPAC01																							
LCDPAC02																							
LCMAC101		3										1											8
LCMAC102																							3
LCMAC103	1																	1	1	1	1	1	17
LCMAC201		1		1				1									1	2	1				11
LCMAC202	1	2							1			1		1	1		1	2	1			1	26
LCIVAC01																							
LCMiAC01					1	1						1		1	1					1			18
LCMiAC02																			2		1		2
Pithovirus sibericum																							
Cedratvirus_A11																							
Orpheovirus		1	1		1	1										1	1						1
Marseillevirus																	1		1				1
Klosneuvirus_KNV1	1	1	1	2	1	1	1	1	3	1	1	1	1	1	1	1	1	2	1	1	1	1	25
mimivirus								1	1						1	1					1		6
Tupanvirus	1	1	1	2	1	1	1	1				1	1	1	1	1	1	2	1	2		1	
<i>C. roenbergensis</i> virus								1								1	1	1	3	1	1	1	16

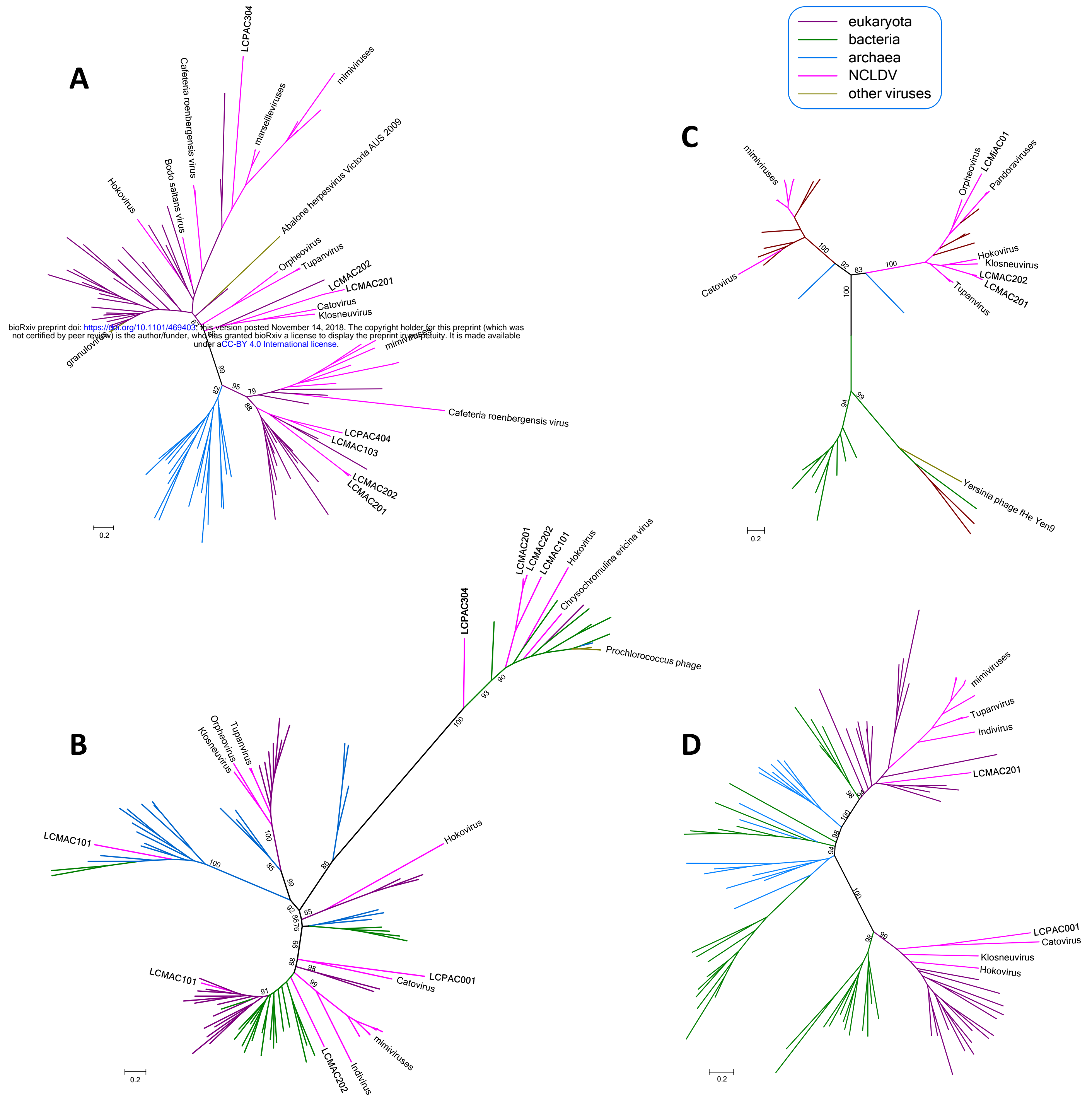
^a translation-related proteins are abbreviated as follows: AlaS, Alanyl-tRNA synthetase; AsnS, Aspartyl/asparaginyl-tRNA synthetase; GlnS, Glutamyl- or glutaminyl-tRNA synthetase; GRS1, Glycyl-tRNA synthetase (class II) ; HisS, Histidyl-tRNA synthetase; IleS, Isoleucyl-tRNA synthetase; MetS, Methionyl-tRNA synthetase; ProS, Prolyl-tRNA synthetase; ThrS, Threonyl-tRNA synthetase; TrpS, Tryptophanyl-tRNA synthetase; TyrS, Tyrosyl-tRNA synthetase; Pth2, Peptidyl-tRNA hydrolase ; eiF1, Translation initiation factor 1 (eIF-1/SUI1); eiF1a, Translation initiation factor 1A/IF-1; eiF2a, Translation initiation factor 2, alpha subunit (eIF-2alpha) ; eiF2b, Translation initiation factor 2, beta subunit (eIF-2beta)/eIF-5 N-terminal domain ; eiF2g, Translation initiation factor 2, gamma subunit (eIF-2gamma; GTPase) ; eiF4e, Translation initiation factor 4E (eIF-4E); eiF5b, Translation initiation factor IF-2 (Initiation Factor 2 (IF2)/ eukaryotic Initiation Factor 5B (eIF5B) family; IF2/eIF5B); eRF1, Peptide chain release factor 1 (eRF1) ; RLI1, Translation initiation factor RLI1

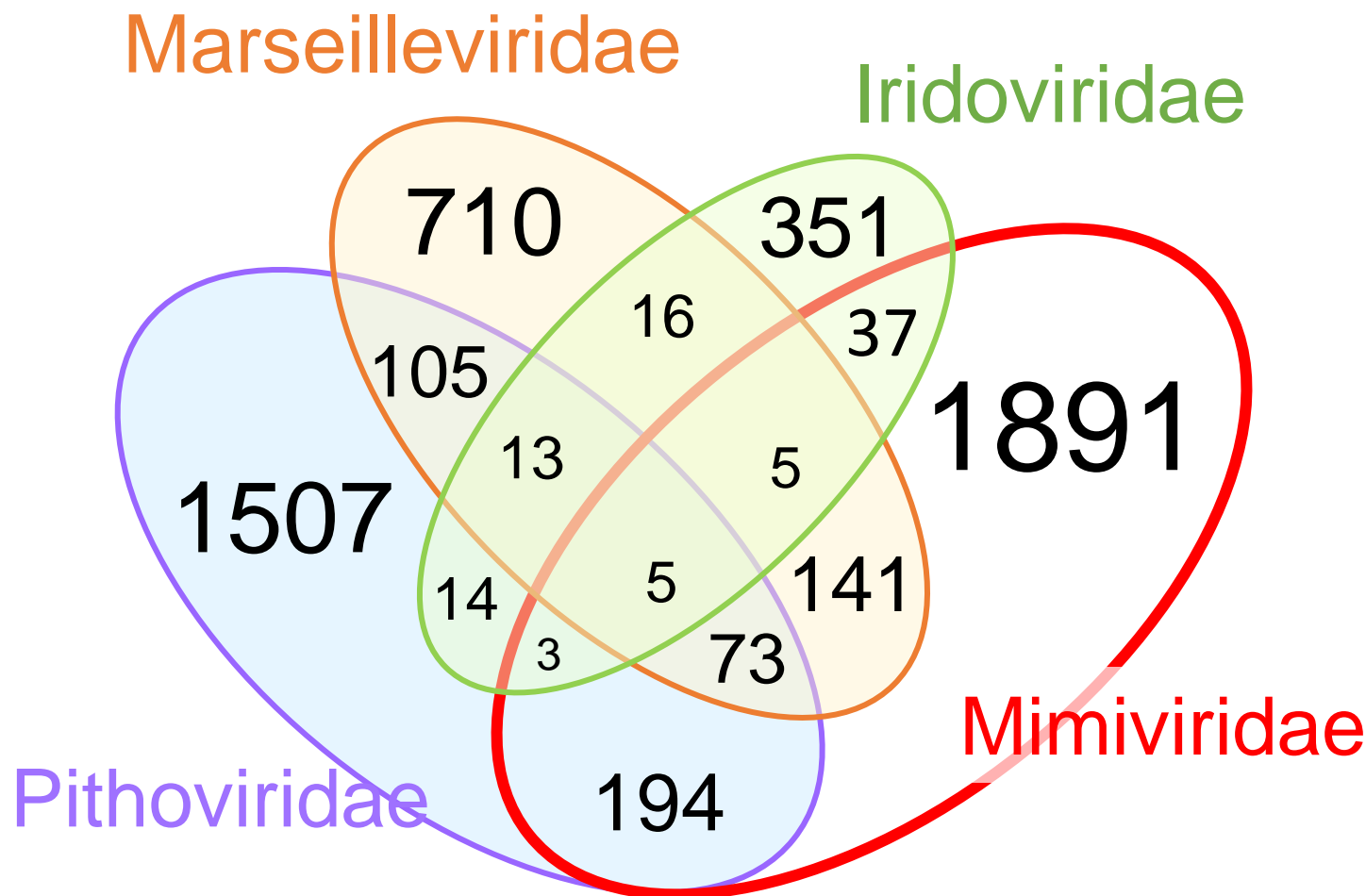
Data for completely sequenced representatives of the relevant NCLDV families are included for comparison.

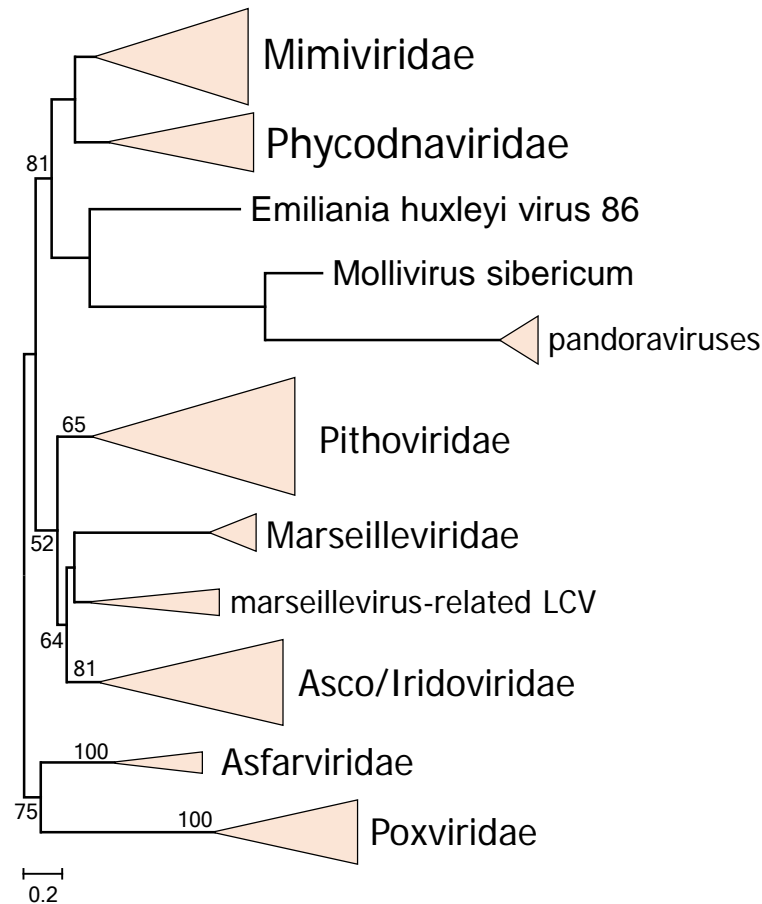


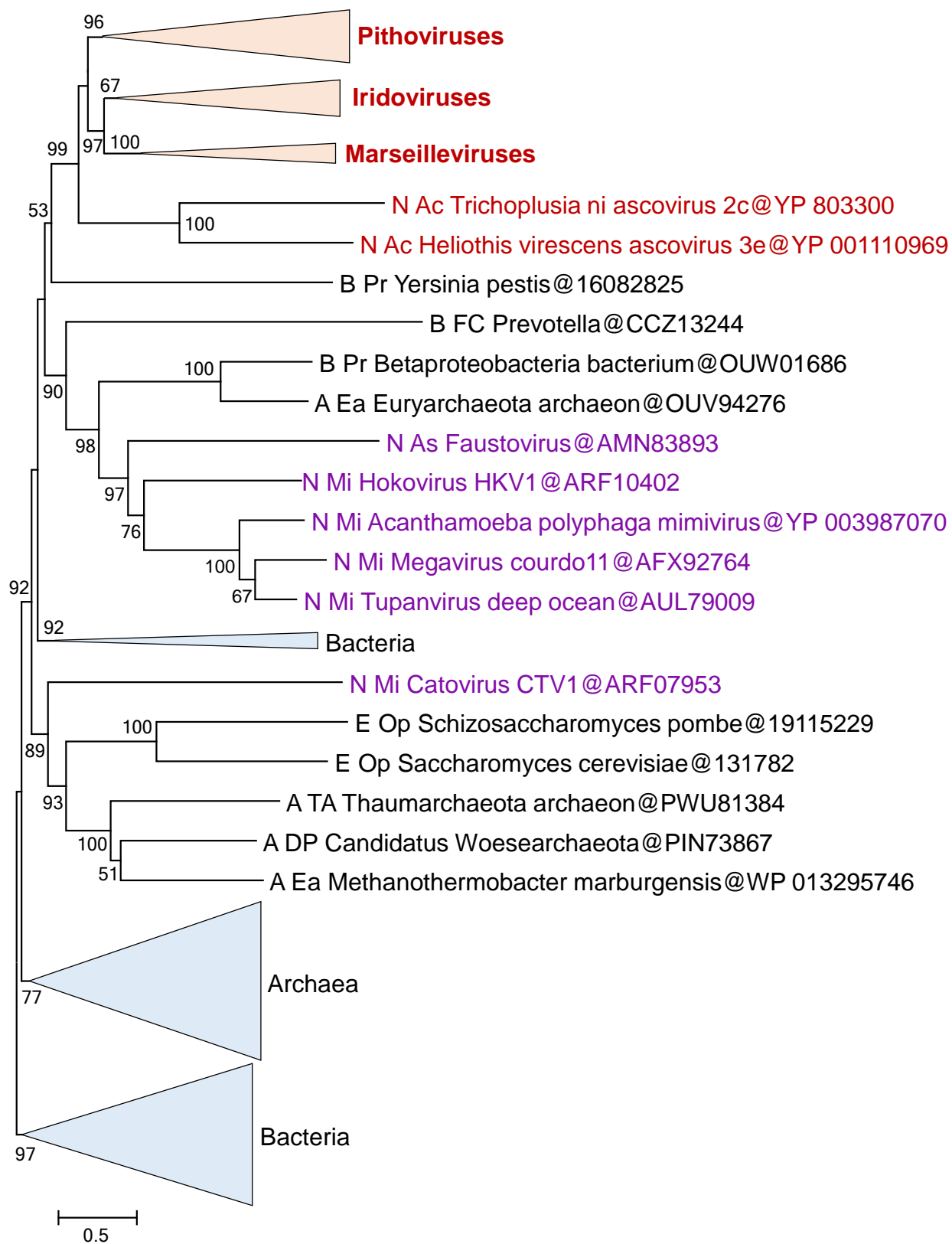


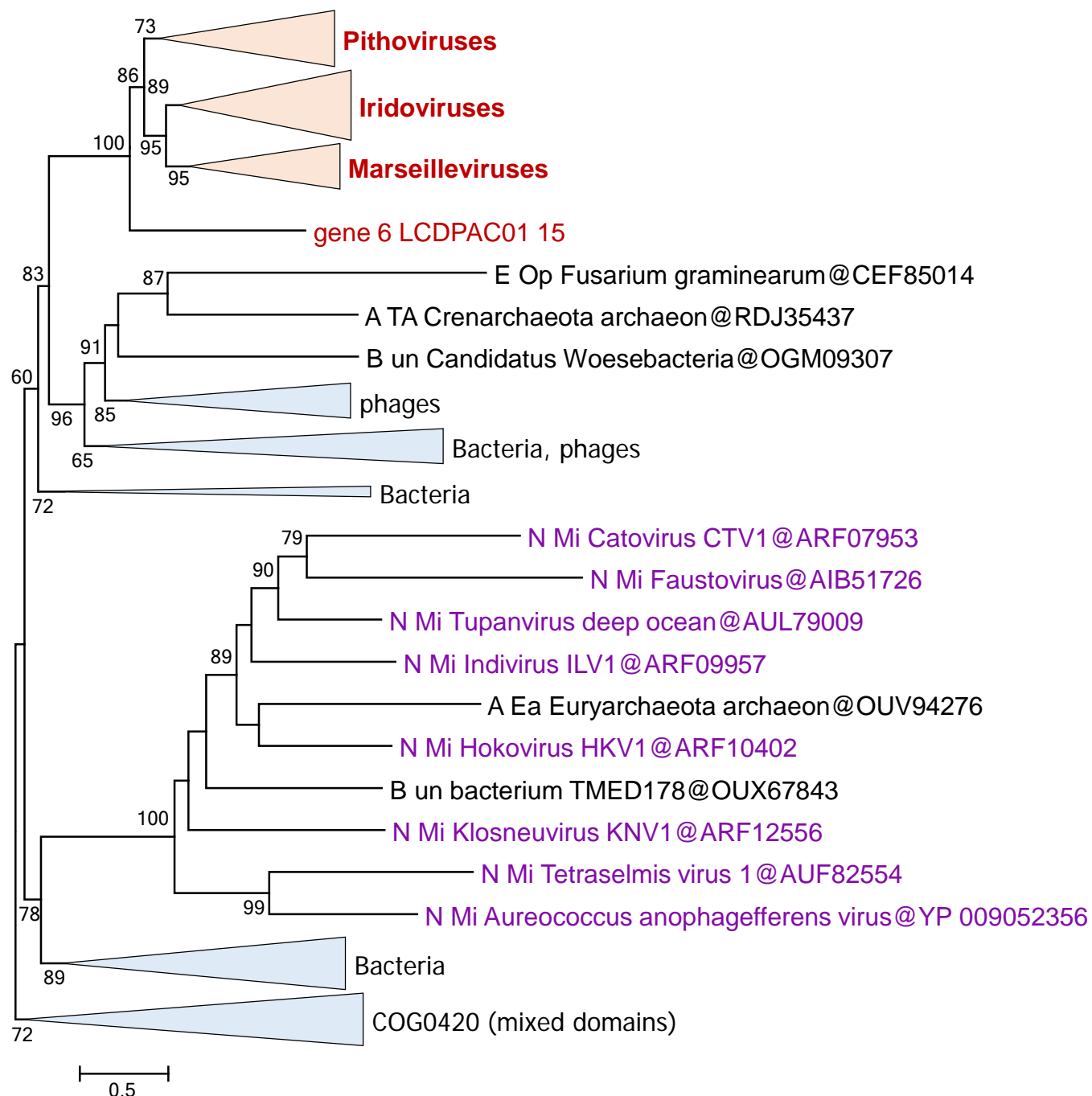




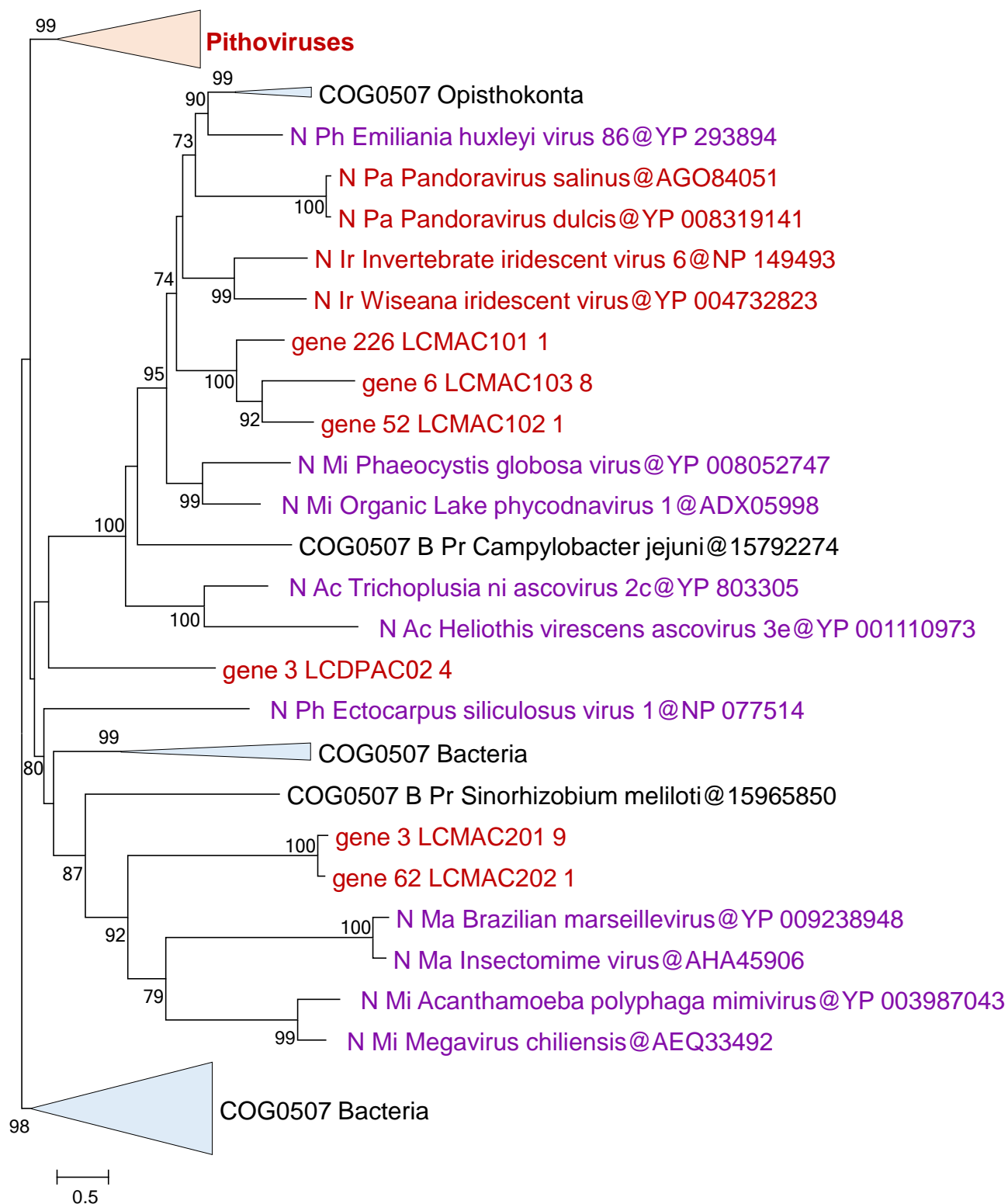




A

B

C



D